CHAPTER IV

RESULTS AND DISCUSSION

4.1 Identification of wood-decaying fungus *D. eschscholzii*

4.1.1 Morphological identification

Description of the species

Daldinia eschscholzii (Ehenb.:Fr.) Rehm.

Stromata turbinate to placentifrom, sessile or with short, stout stipe, solitary to infrequently aggregated, smooth, 1.54-4 cm diam × 1-4 cm high; surface brown vinaceous, dark brick, sepia, grayish sepia, or vinaceous gray, blackened and varnished in age; dull reddish brown granules immediately beneath surface, with KOH-extractable pigments livid purple, dark livid, or vinaceous purple; the tissue between perithecia brown, pithy to woody; the tissue below the perithecial layer compose of alternating zones, the darker zones dark brown, pithy to woody, 1-0.2 mm thick, the lighter zones white, grey, or grayish brown, gelatinous and very hard when dry becoming pithy to woody, persistent, 0.3-1 mm tick.

Perithecia tubular, 0.8-1.5 mm high × 0.3-0.4 mm diam.

Ostioles obsolete or slightly papillate.

Asci 160-195 μm total length × 7-9 μm broad, the spore-bearing part 70-80 μm long, the stipe 90-120 μm long, with apical apparatus, discoid, 0.5 μm high × 2-2.5 μm broad, blueing in Melzer' reagent.

Ascospores brown to dark brown, unicellular, ellipsoid-inequilateral, with narrowly rounded ends, 11.3-13.8 × 5-6.3 μm, with straight germ slit spore-length on convex side; perispore dehiscent in 10% KOH, conspicuous coil ornamentation; epispore smooth.

Cultural characteristics and anamorph

Colonies growing rapidly on potato dextrose agar (PDA), becoming brown grey and granular as conidia are produced, dark brown with green on the underside, prolific conidial promotion, conidiophores and conidia very similar to those described by Ju *et al.* (1997). Classical identification of fungi is based on observe characteristics. Assignment of morphological species can be based on colony surface texture, hyphal pigments, exudates, margin shapes, growth rates, and sporulating structures (Redlin and Carris, 1996). This fungal was identified as belonging to the genus *Daldinia.* Colony characteristic on PDA and light microscopic characteristic of *D. eschscholzii* are shown in Figure 4.1. Scanning Electron Microscopic characteristic of *D. eschscholzii* are shown in Figure 4.2.

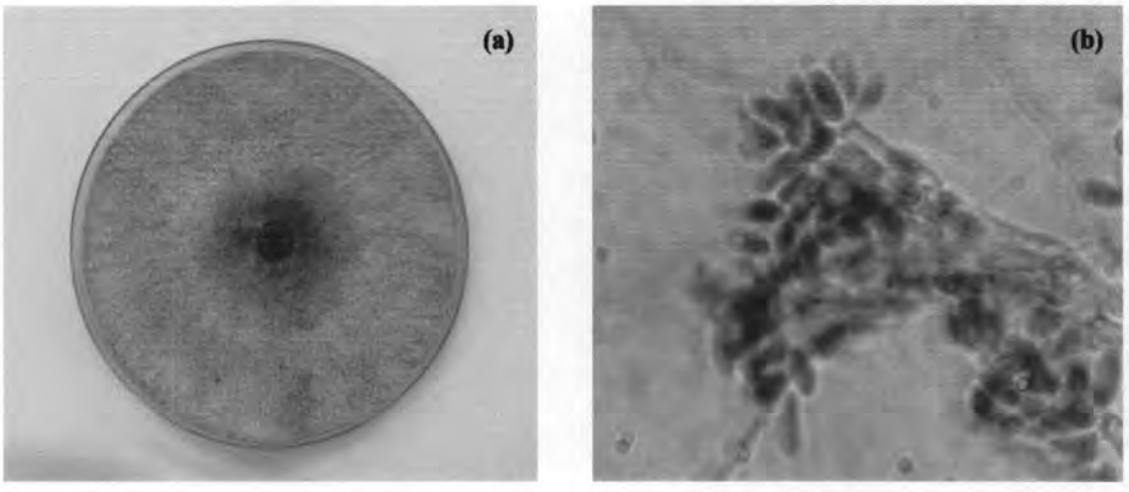

Figure 4.1 Colonial and microscopic characteristic of *D. eschscholzii.* (a); cultured on PDA showing the pale brown grey colony, (b); lactophenol cotton blue mount at magnification ×1,000 of the fungal mycelia and conidial showing irregularly branched conidiophores, with denticles closely crowded of the conidia, and deposits of a brown material on the conidiophore

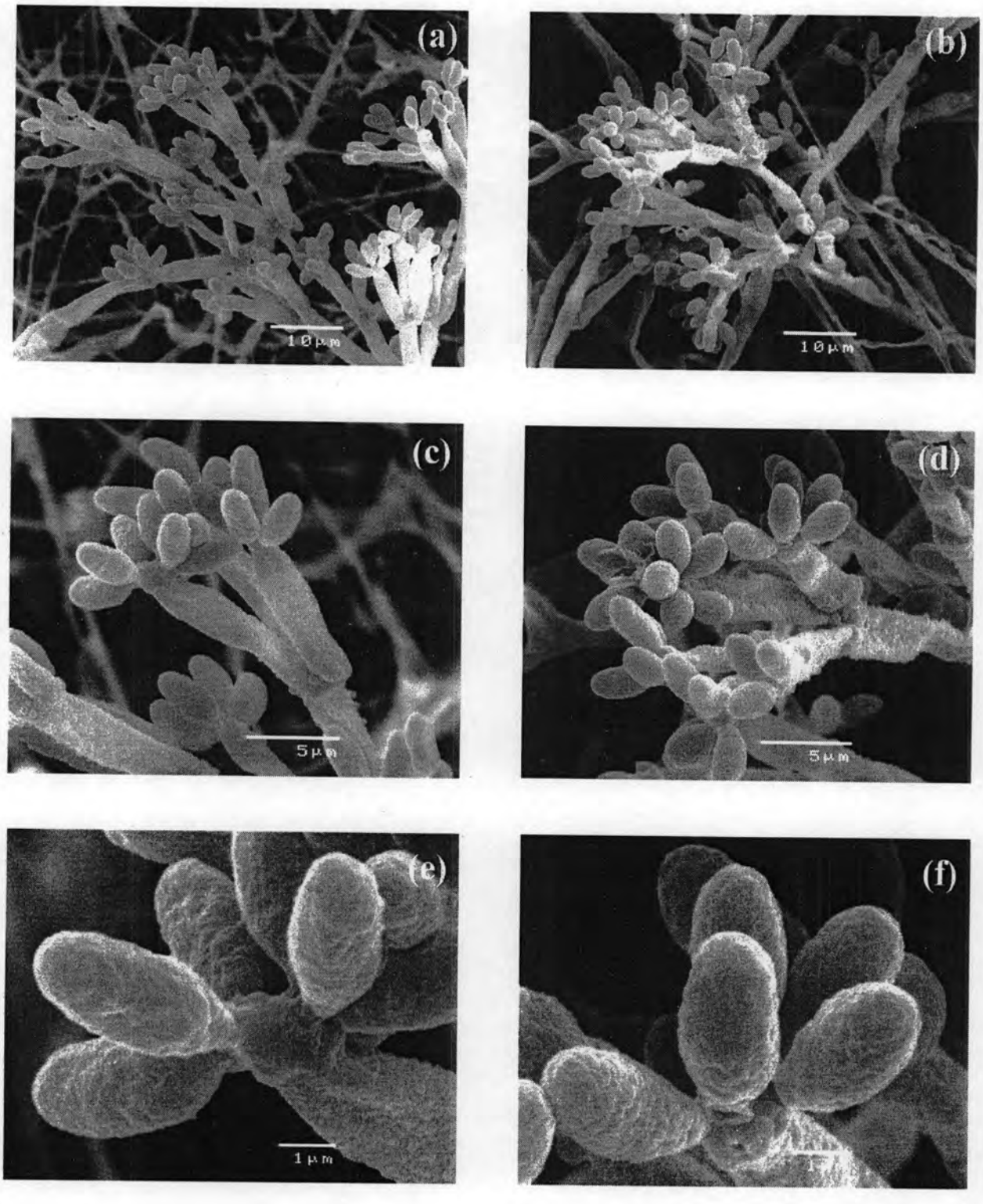

Figure 4.2 Scanning Electron Microscopic characteristics of *D. eschscholzii*. (a, b); irregularly branched conidiophores (bar = 10 µm), (c, d); closely crowded conidia at the tip of the conidiogenous cell (bar = 5 µm), and (e, f); single conidia (bar = 1µm) with scaled on conidiophores

Induction of teleomorph formation

Taxonomic studies on xylariaceous fungi have focused mainly on the teleomorph stage. Cultural studies are frequently undertaken whenever possible to study anamorph-teleomorph connections. On the other hand studies on the anamorph stage are often resticed to selected genera such as *Biscogniauxia*, *Daldinia*, *Hypoxylon*, *Rosellinia*, or *Xylaria*. Even with information on the anamoph identification to species is very usually very difficult and furthermore in many genera only fragmentary information is available (Petrini and Rodrigues, 1995). Species of *Daldinia*, along with an increasing number of the Xylariaceae, are suggested to be common endophytes occurring in a diverse range of host plants in which they fail to produce a teleomorph (Petrini and Petrini, 1985; Griffith and Boddy, 1990; and Petrini *et al.*, 1995). This indicates a broader host range than reflected by the collections of stromata. However, anamorphs of the closely related *Daldinia* spp. produced in the culture can be difficult to identify to the species level because, so far, the cultural characteristics have been described for only a limited number of species and the interpretations of taxa is somewhat confused (Petrini and Petrini, 1985; Petrini and Muller, 1986; and Johannesson *et al.*, 2000).

In an attempt to resolve identification problems a technique to induce the production of the sexual state by incubation of pure culture into sterilized stem sections of mango wood, followed by incubation under controlled conditions in the laboratory or incubation in the field has also been undertaken. In this study, *D. eschscholzii* developed to maturity (Figure 4.3). Moisture is a very important ecological condition required by most xylariaceous fungi, because a moist habitat is essential for mycelial growth and development of fruiting structures (Petrini and Rodrigues, 1995). Mekkamol (1998) found that sometimes when inoculated wood was transferred to the forest they failed to develop further because the specimens dried out, were destroyed by termites, or taken by monkeys. However, by placing inoculated twigs in damp sand either in bags, open or sealed, or in earthware pots it was possible to produce mature stromata.

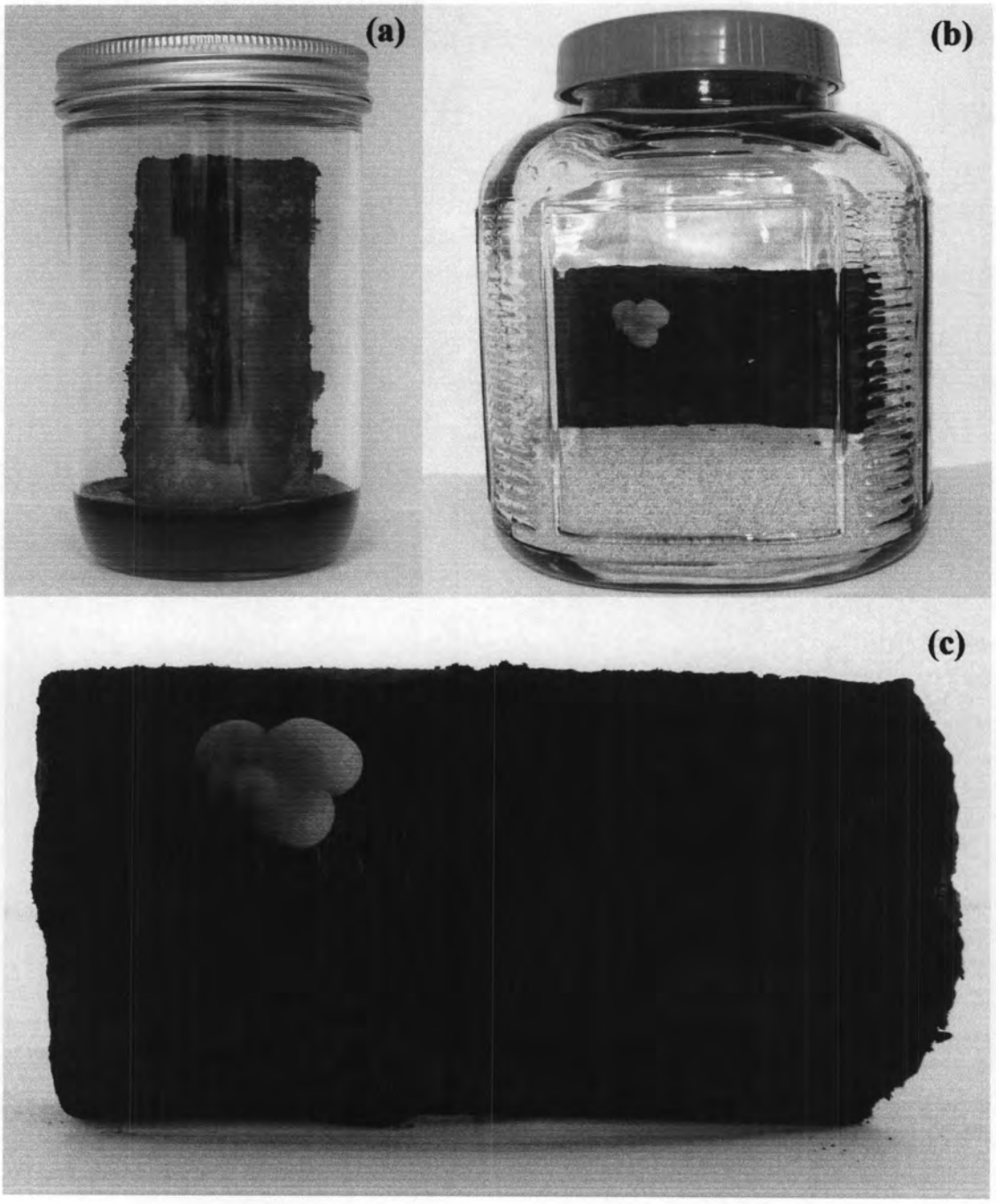

Figure 4.3 Induction of *D. eschscholzii* teleomorph formation. (a); Culture of *D. eschscholzii* inoculated in mango twig inoculated in glass jar. (b, c); Mature teleomorphic stroma on mango twig inoculated in damp sand for 6 months

D. eschscholzii is widely distributed throughout Thailand and is certainly the most frequently collected species. It is found throughout South East Asia and appears common throughout the tropics and subtropics. It has long been considered to be the tropical equivalent of *D. concentrica* and ranked as a variety (Dennis, 1963, Dennis, 1974, and Thind and Dargan, 1978). There are, however, clear separating feature. Ascospores of *D. eschscholzii* have an ornamented perispore which appear to have transversly oriented fibrils by SEM whereas those of *D. concentrica* are smooth. The stromata in *D. eschscholzii* are also usually smaller with a smoother surface than *D. concentrica* (Van der Gucht, 1995). Ju *et al.* (1997) also demonstrated that the KOH extractable pigments in *D. eschscholzii* are purplish but those from *D. concentrica* are yellowish, greenish to olivaceous. There are also cultural differences (Ju *et al.*, 1997). Table 4.1 gives an overview on their characteristics in comparison with authentic and type materials of *D. concentrica,* and *D. eschscholzii.*

One of the largest and most conspicuous genera of the Xylariaceae, *Daldinia*, is not well represented in Thailand and on current data does not seem especially common there. *D. eschscholzii* is the only species which can be considered widespread but it is not often found in natural forest unless in a clearing or at the forest edge (Thienhirun, 1997).

Table 4.1 Teleomorphic and amamorphic characteristics of *D. concentrica* and *D. eschscholzii*

Species	Occureence	Hosts	Ascospore size (μm)	Ascospores (SEM)	Ascal apical ring (μm)	Type and size(μm) of conidiophores	Conidiogenous cells (μm) and type of conidiogenesis	Conidia (μm)
D. concentrica	Europe	*Fraxinus* (preferred) *Fagus, Ulmus, Salix*	13-16(-17) × 6-7.5[a]	faint ridges (at > 10,000×)	0.3-0.5×3-3.5[a]	*Nodulisporium*-like, 100-200 × 3.5-4	10-25 × 3-4, holoblastic	(5.5)6.5-8(9) × 3.5-4.5
D. eschscholzii	Pantropical, originating from Asia	no apparent host specific	10-14(-15.5) × 5-6 (-6.5)[b]	conspicuous transverse (at 5,000×)	0.5×2-2.5[b]	*Nodulisporium*-like, 100-200 × 3-3.5	8-25 × 2-3, holoblastic	4.5-6.5 × 2.5-3

[a]Anamorphic branching patterns as defined in Ju and Roger (1996)

[b]Our measurement, basically in agreement with Ju *et al.* (1997)

4.1.2 Molecular Identification

D. escheschol zii was sent for identification by molecular methods at the Macrogen, Seoul, Korea The rDNA ITS region of *D. escheschol zii* was amplified with the conserved fungal primer ITS_{1F} and ITS_4. *D. escheschol zii* produced a single ITS band. The length of corresponding fragment was 584 bp, containing a part of the 18S, ITS1, 5.8S and 28S rDNA is shown in Figure 4.4.

```
    1
5'  AGAGGGCTCG    TTGGTGACCA    GCGGAGGGAT    CATTACTGAG
    TTATCTAAAC    TCCAACCCTA    TGTGAACTTA    CCGCCGTTGC
    CTCGGCGGGC    CGCGTTCGCC    CTGTAGTTTA    CTACCTGGCG
    GCGCGCTACA    GGCCCGCCGG    TGGACTGCTA    AACTCTGTTA
    TATATACGTA    TCTCTGAATG    CTTCAACTTA    ATAAGTTAAA
    ACTTTCAACA    ACGGATCTCT    TGGTTCTGGC    ATCGATGAAG
    AACGCAGCGA    AATGCGATAA    GTAATGTGAA    TTGCAGAATT
    CAGTGAATCA    TCGAATCTTT    GAACGCACAT    TGCGCCCATT
    AGTATTCTAG    TGGGCATGCC    TGTTCGAGCG    TCATTTCAAC
    CCTTAAGCCC    CTGTTGCTTA    GCGTTGGGAA    TCTAGGTCCC
    CAGGGCCTAG    TTCCCCAAAG    TCATCGGCGG    AGTCGGAGCG
    TACTCTCAGC    GTAGTAATAC    CATTCTCGCT    TTTGCAGTAG
    CCCCGGCGGC    TTGCCGTAAA    ACCCCTATAT    CTTTAGTGGT
    TGACCTCGAA    TCAGGTAGGA    ATACCCGCTG    AACTTAAGCA
    TATCAATAAG    NCGGGAGGAA    AANN 3'
                                  584
```

Figure 4.4 Nucleotide sequences of *D. escheschol zii*, containing a partial sequence of the 18S, ITS1, 5.8S and 28S rDNA

A blast search was performed to find a similar sequence to ITS region of fungal isolate LSS6 in the Genbank DNA database, available from: http://www.ddbj.nig.ac.jp. The results revealed that ITS region of *D. escheschol zii* had 99% identity to *D. escheschol zii*, as showed in Figure 4.5. The nucleotide sequence data reported will appear in the DDBJ/EMBL/GenBank nucleotide sequence databases with the accession number AB284189.

gb|DQ322086.1| *Daldinia eschscholzii* isolate SUT168 internal transcribed spacer 1, 5.8S ribosomal RNA gene, and internal transcribed spacer 2, complete sequence; and 28S ribosomal RNA gene, partial sequence

Length = 534, Score = 981 bits (531),

Expect = 0.0, Identities = 533/534 (99%),

Gaps = 0/534 (0%)

Strand=Plus/Plus

```
Query  36   CTGAGTTATCTAAACTCCAACCCTATGTGAACTTACCGCCGTTGCCTCGGCGGGCCGCGT  95
            ||||||||||||||||||||||||||||||||||||||||||||||||||||||||||||
Sbjct  1    CTGAGTTATCTAAACTCCAACCCTATGTGAACTTACCGCCGTTGCCTCGGCGGGCCGCGT  60

Query  96   TCGCCCTGTAGTTTACTACCTGGCGGCGCGCTACAGGCCCGCCGGTGGACTGCTAAACTC  155
            ||||||||||||||||||||||||||||||||||||||||||||||||||||||||||||
Sbjct  61   TCGCCCTGTAGTTTACTACCTGGCGGCGCGCTACAGGCCCGCCGGTGGACTGCTAAACTC  120

Query  156  TGTTATATATACGTATCTCTGAATGCTTCAACTTAATAAGTTAAAACTTTCAACAACGGA  215
            ||||||||||||||||||||||||||||||||||||||||||||||||||||||||||||
Sbjct  121  TGTTATATATACGTATCTCTGAATGCTTCAACTTAATAAGTTAAAACTTTCAACAACGGA  180

Query  216  TCTCTTGGTTCTGGCATCGATGAAGAACGCAGCGAAATGCGATAAGTAATGTGAATTGCA  275
            ||||||||||||||||||||||||||||||||||||||||||||||||||||||||||||
Sbjct  181  TCTCTTGGTTCTGGCATCGATGAAGAACGCAGCGAAATGCGATAAGTAATGTGAATTGCA  240

Query  276  GAATTCAGTGAATCATCGAATCTTTGAACGCACATTGCGCCCATTAGTATTCTAGTGGGC  335
            ||||||||||||||||||||||||||||||||||||||||||||||||||||||||||||
Sbjct  241  GAATTCAGTGAATCATCGAATCTTTGAACGCACATTGCGCCCATTAGTATTCTAGTGGGC  300

Query  336  ATGCCTGTTCGAGCGTCATTTCAACCCTTAAGCCCCTGTTGCTTAGCGTTGGGAATCTAG  395
            ||||||||||||||||||||||||||||||||||||||||||||||||||||||||||||
Sbjct  301  ATGCCTGTTCGAGCGTCATTTCAACCCTTAAGCCCCTGTTGCTTAGCGTTGGGAATCTAG  360

Query  396  GTCCCCAGGGCCTAGTTCCCCAAAGTCATCGGCGGAGTCGGAGCGTACTCTCAGCGTAGT  455
            ||| ||||||||||||||||||||||||||||||||||||||||||||||||||||||||
Sbjct  361  GTCTCCAGGGCCTAGTTCCCCAAAGTCATCGGCGGAGTCGGAGCGTACTCTCAGCGTAGT  420

Query  456  AATACCATTCTCGCTTTTGCAGTAGCCCCGGCGGCTTGCCGTAAAACCCCTATATCTTTA  515
            ||||||||||||||||||||||||||||||||||||||||||||||||||||||||||||
Sbjct  421  AATACCATTCTCGCTTTTGCAGTAGCCCCGGCGGCTTGCCGTAAAACCCCTATATCTTTA  480

Query  516  GTGGTTGACCTCGAATCAGGTAGGAATACCCGCTGAACTTAAGCATATCAATAA  569
            ||||||||||||||||||||||||||||||||||||||||||||||||||||||
Sbjct  481  GTGGTTGACCTCGAATCAGGTAGGAATACCCGCTGAACTTAAGCATATCAATAA  534
```

Figure 4.5 Alignment data of a part of the 18S, ITS1, 5.8S and 28S rDNA of *D. eschescholzii* and reference 1 taxa

A molecular method of identification was also performed. The nucleotide sequence of the ITS region of rDNA is conserved. It can be used to delineate species relationships and separated taxonomy from class to species (Mitchell *et al.*, 1995). The nucleotide sequence of the ITS region of *D. eschscholzii* was similar to 99% identity of *D. eschscholzii* reported by Suwanasai *et al.*, 2005.

4.2 Wood decay activity by *D. eschscholzii*

The use of an *in vitro* natural wood substrate to monitor wood decay is most suitable to represent what happens in nature. Previous wood decay tests have employed wood mass loss estimation (Vrijmoed and Hodgkiss, 1988; Zare-Maivan and Shearer, 1998a, 1998b; Worrall *et al.*, 1997; and Yuen *et al.*, 1999). In this study, wood decay by *D. eschscholzii* gave weight losses on *T. grandis* from 5.3-28.5% after 3 months. The decay of *T. grandis* wood compared with control wood showed in Figure 4.6. The weight losses reported here for *D. eschscholzii* compares with data reported by others workers (Table 4.2)

Table 4.2 Weight losses of various timbers by xylariaceous fungi

Reference	Wood species	Range of % weight loss	Weeks exposure
Lee, 1997	Beech	17.9-73.6	24
Abe, 1990	Aspen	8.6-56.1	24
Nilsson *et al.*, 1989	Bisch	14.9-76.6	16
Boddy *et al.*, 1989	Ash	6.5-29.9	56-204
Cartwright and Findlay, 1946	Beech	14	16
Merrill *et al.*, 1964	Aspen and Red oak	10-26	12
Rajagopalan, 1966	Aspen	16	12
This study	Teak	5.3-28.5	12

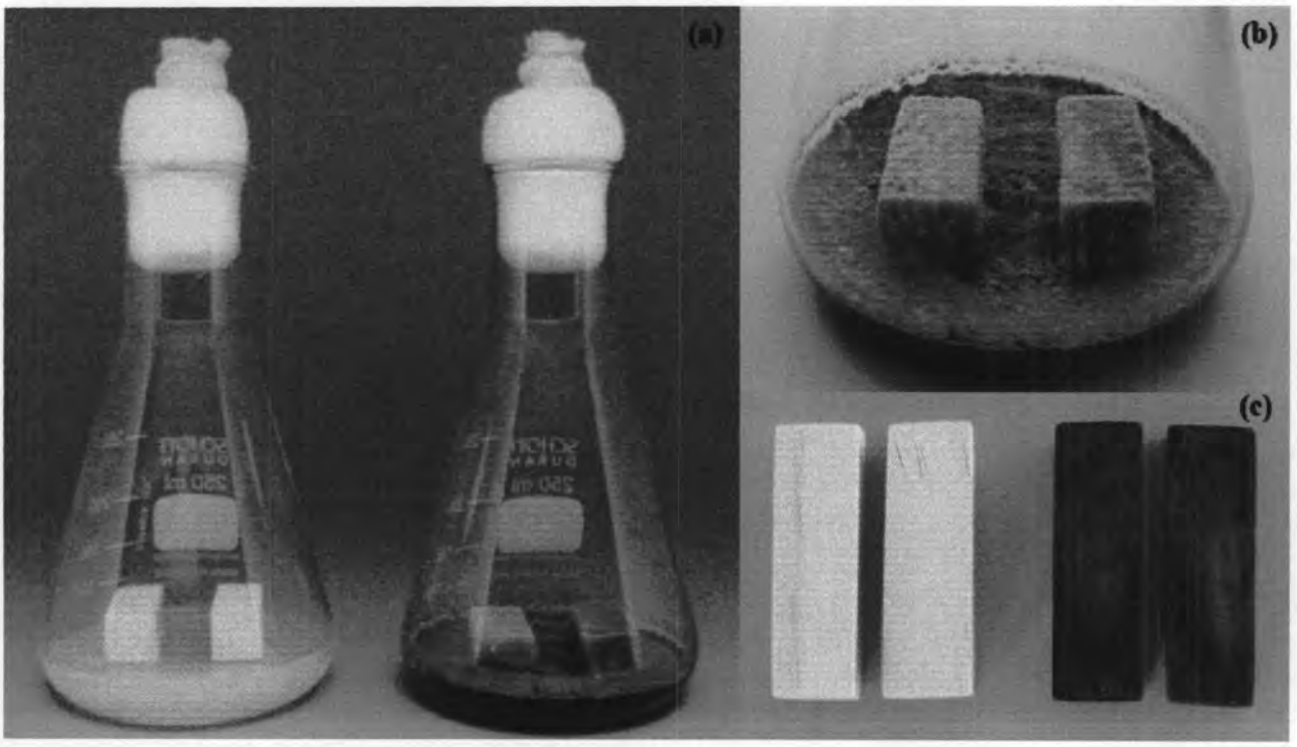

Figure 4.6 Set up of wood decay experiment. (a); Growth of *D. eschescholzii* on *T. grandis* wood, left; control, right; experiment, (b); *D. eschescholzii* on *T. grandis* wood after 3 months, and (c); Comparison of *T. grandis* wood blocks before and after decay by *D. eschescholzii*

T. grandis wood blocks were quickly colonized by *D. eschescholzii* with formation of an abundant black mycelium mass. Decayed wood blocks were soft, fibrous, and broke easily into fragments on a longitudinal plane. In the control *T. grandis* wood blocks (Figure 4.7; a, b), a cross-field zone and aerolate pits with characteristic circular borders are apparent. The regular pits observed in the SEM of control wood samples became larger and irregular. Large masses of mycelium were found in cells with simultaneous degradation (Figure 4.7; c, d), while in the decayed areas were scarce. The fiber cell walls had no middle lamella and cells were loosely arranged. A simultaneous decay of all cell wall components was found in cells from these areas, erosion through and holes were evident. The cell wall was attacked from the lumen toward the middle lamella, and the wall layers were eroded in a localized area (Figure 4.7; e-h). As collapse of eroded areas occurred, the fungus filled these voids with mycelia.

The infection process and wood decay by *D. eschscholzii* in *T. grandis* described in this work could be similar to what is happening in other trees, which needs to be confirmed (Chapela and Boddy, 1988a and Chapela and Boddy, 1988b; Baum *et al.*, 2003). The results obtained in our study suggest the hypothesis that within the lifecycle of some wood decays fungi.

Xylariaceous taxa are known to colonize and decay wood, and because they are ascomycetes it has been assumed that they carry out soft-rot type decay. Soft-rot decay features have been observed for several xylariaceous taxa (Francis and Leightley, 1984; and Worral *et al.*, 1997). Their ability to degrade wood polyoses has also been demonstrated by chemical analysis of decayed Japanese Oak (*Quercus serrata*) (Abe, 1989), and mineralization of radiolabelled glucans incorporated into Norway maple (*Acerplatanoides*) twigs (Sutherland and Crawford, 1981). *In vitro* studies have also shown that both *Xylaria* and *Hypoxylon* species are capable of producing cellulolytic enzymes. *Xylaria anisopleura* and *Xylaria regalis* have been shown to produce endoglucanase and cellobiohydrolase at levels comparable to the well-known cellulolytic fungus *Trichoderma reesei* (Wei *et al.*, 1992). In an ecological context, however, this is not surprising for such wood-decaying fungi, since these polysaccharides are required as a primary carbon source for growth.

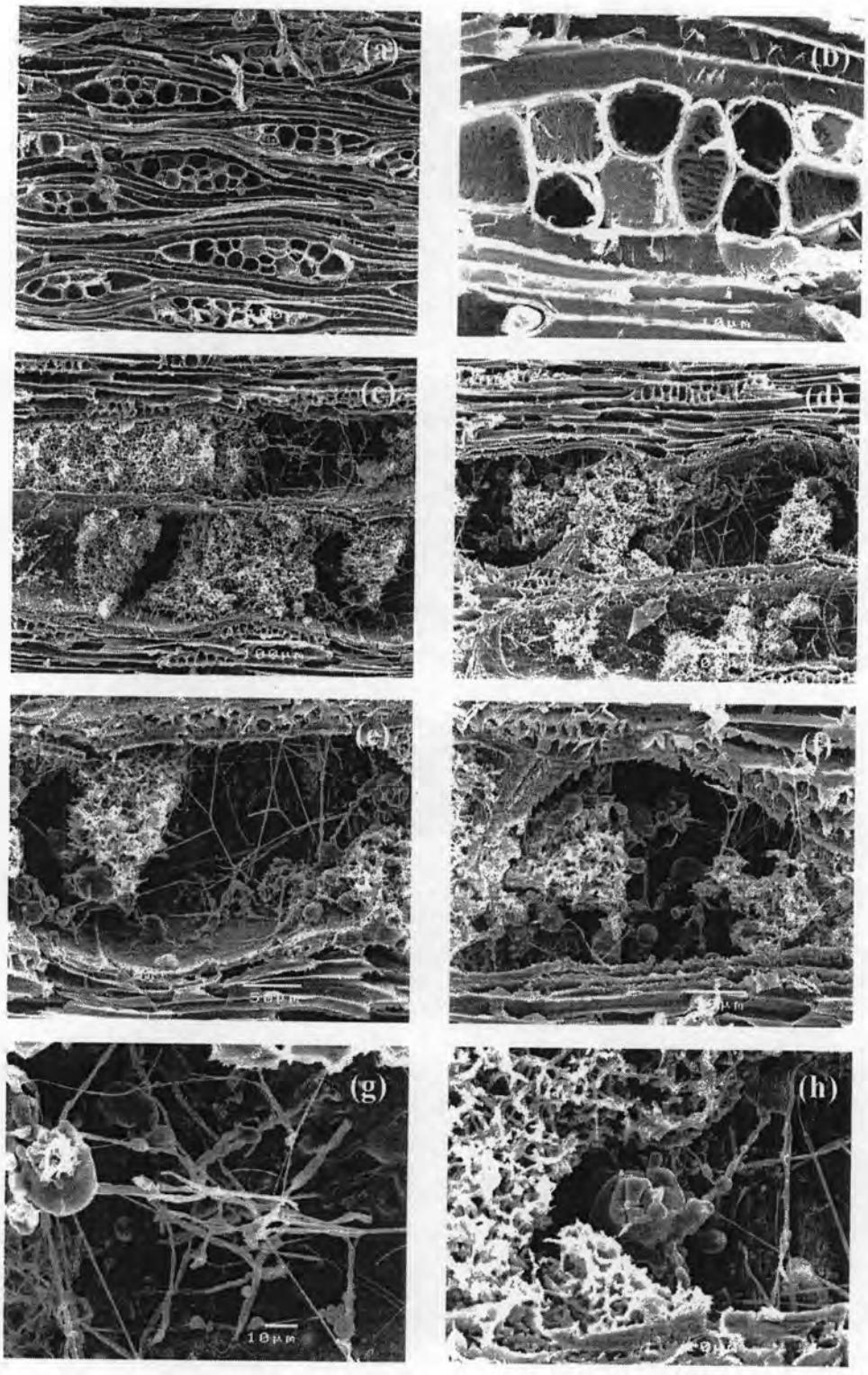

Figure 4.7 *Tectona grandis* decay caused by *D. escheschollzii*. (a, b); Longitudinal section of *T. grandis* (bar = 100 μm, and 10 μm), (c, d); Simultaneous wood decay characterized by strong degradation of all cell-wall components, including abundant mycelium inside (bar = 100 μm, and 10 μm), and (e, f); A simultaneous removal of all cell wall components results in large cavities (bar = 50 μm), and (g, h); As the voids in the wood form, mycelia fill the space (bar = 10 μm)

4.3 Cellulolytic enzyme activities on solid media

Solid media enzyme assays detect enzyme synthesis, their release from the mycelium, and activity in the medium following production. *D. eschscholzii* was capable of cellulose degradation as shown by downward dye diffusion in the clear agar layer due to release of azure dye from cellulose (Figure 4.8 a). Although this method was designed as a qualitative test, it can be used during screening procedures to estimate relative cellulolytic ability by comparison with fungi known to be highly active in the degradation of cellulose. Cellulose-azure has been widely used for cellulolytic activity measurement by different research groups (Hotten *et al.*, 1981; Palmisano *et al.*, 1993; and Adney *et al.*, 1989). Endoglucanase activity was shown by using CMC as the substrate, and a clear zone was observed (Figure 4.8 b,). The esculin agar was specially designed to screen β-glucosidase production from most of fungi (Pointing, 1999). *D. eschscholzii* can produced a strong dark-brown colour zone in the media (Figure 4.8 c).

Wood-decaying fungi are the most important microorganisms that can colonize and degrade wood (Zabel and Morell, 1992) by attacking cell components using enzyms (Kirk *et al.*, 1980; and Kirk and Farrell, 1987). The production of cellulolytic enzymes is interesting. Carroll and Petrni (1981) suggested that this fungus may be latent pathogens or vigorous decomposer after plant death. These taxa maybe dominant in the leaves until plant death, and the evidence here indicates that they may then adopt a saprobic lifestyle and degrade dead leaves and possibly wood.

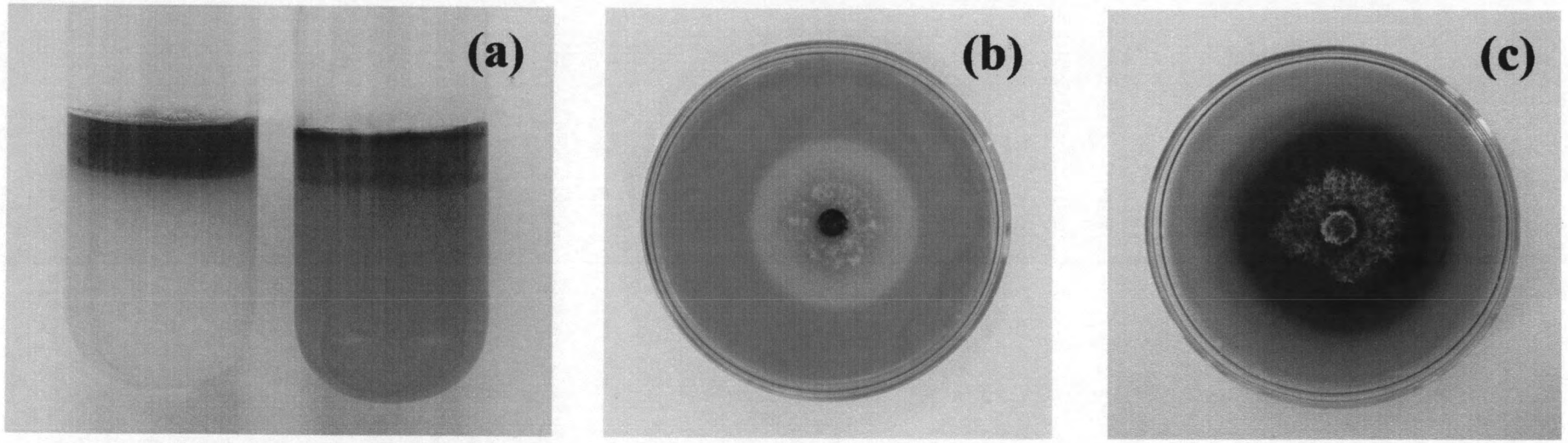

Figure 4.8 Cellulolytic enzyme activities on solid media. (a); Typical colour-reactions observed in the Cellulose azure agar test, the control represents an un-inoculated bottle, (b); A Congo red stained plate containing 1% of CMC; and (c); A black color developed in the medium by *D. eschscholzii* producing β-glucosidase

4.4 Culture conditions and production of β-glucosidase

A number of different carbon sources were tested in growth experiments for their ability to promote the development of fungal mycelium and stimulate the secretion of cellulolytic enzymes. Carboxy-methylcellulose (CMC) was the most effective inducer of β-glucosidase activity of the carbon sources tested. Microcrystalline cellulose (Avicel® PH-101) and filter paper were also fairly good inducers but with glucose as a carbon source enzyme production was repressed (Figure 4.9). The low activity in glucose cultures indicates that the main part of β-glucosidase activity is under catabolite repression while a small part may be constitutive. The highest level of total β-glucosidase activity (8.102 U/ml) was produced in CMC after 10 days growth.

Previous workers reported that β-glucosidases are inducible enzymes (Kubicek, 1992, 1993). They can be induced with different inducers such as cellobiose, lactose and sophorose (Mandels and Reese, 1960; and Mandels *et al.*, 1962). However, most of the microorganisms have produced highest levels of β-glucosidase when grown on cellulose (Ryu and Mandels, 1980). Other researchers reported that several fungi were found to produce β-glucosidases on different carbohydrates as a carbon sources (Pou *et al.*, 1988; Saha and Bothast, 1996), and multiple forms of β-glucosidases have been found in the culture broth of a variety of microorganism (Takashima *et al.*, 1996; Christakopoulos *et al.*, 1994; Lymar *et al.*, 1995; Cai *et al.*, 1998).

This result is interesting due to the fact that CMC is a highly purified synthetic substrate, becoming expensive for large-scale enzyme production. The utilization of agro-industrial residues as potential substrates for the production of β-glucosidases and other component (endoglucanase, cellobiohydrolase), hemicellulase and pectinase has attracted much attention (Hang *et al.*, 1994; Romeo *et al.*, 1999., and Krishna *et al.*, 1999) since it can contribute to lower the costs of enzyme production and also to reduce the environmental pollution caused by the accumulation of lignocellulosic wastes.

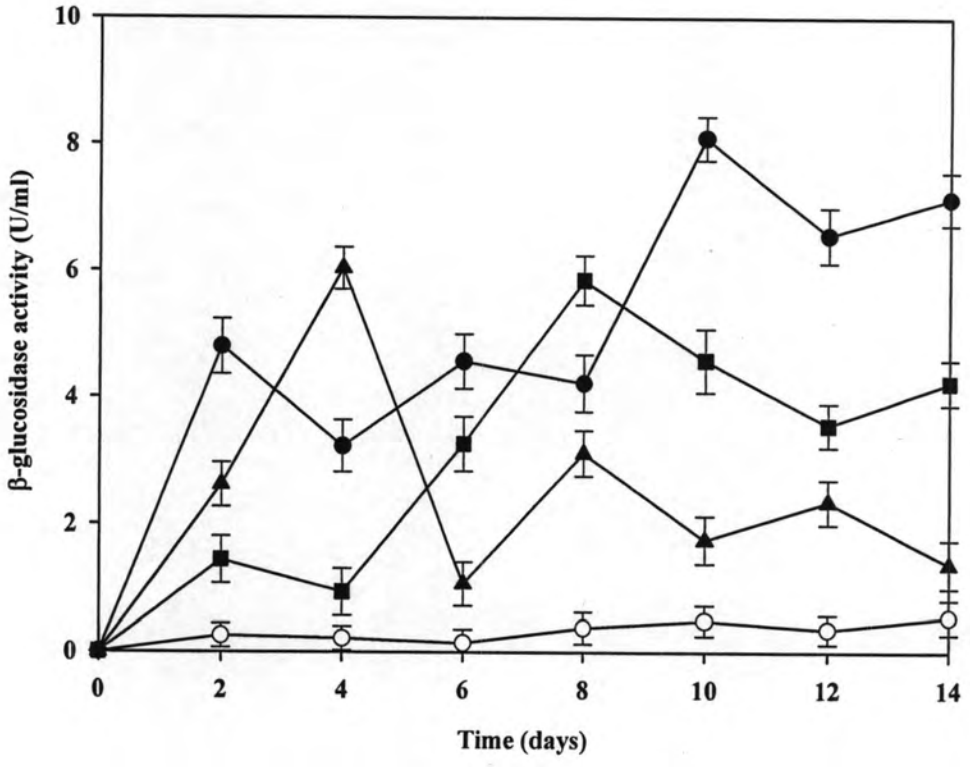

Figure 4.9 Time course of β-glucosidase production by *D. eschscholzii* grown on different carbon source. Values represent the average of three replicate experiments. Error bars represent the standard deviation. Carboxymethyl-cellulose (●); filter paper (▲); Avicel® PH-101 (■); and glucose (○)

4.5 Purification of β-glucosidase from *D. eschscholzii*

4.5.1 Step of enzyme purification

The development of techniques and methods for the separation and purification of proteins has been an essential pre-requisite for many of the recent advancements in bioscience and biotechnology research. The global aim of a protein purification process is not only the removal of unwanted contamination, but also the concentration of the desired protein and its transfer to an environment where it is stable and in a form ready for the intended application (Queiroz *et al.*, 2001). The principle properties of the enzymes that can be exploited in separation methods are size, charge, solubility and the possession of specific binding sites (Queiroz *et al.*, 2001; and Amersham Pharmacia Biotechnol, 1999). Most purification protocols require more than one step to achieve the desired level of product purity. Hence, the key to successful and efficient protein purification is to select the most appropriate techniques, optimize their performance to suit the requirements and combine them in a logical way to maximize yield and minimize the number of step required (Amersham Pharmacia Biotechnol, 1999).

An extracellular β-glucosidase was purified to homogeneity from the culture filtrate of *D. eschscholzii* grown on CMC growth medium. β-glucosidase was successfully purified through ammonium sulfate precipitation, SP Sepharose, Phenyl Sepharose, and Superdex-200 column chromatography. Upon fractionation of the β-glucosidase active fraction with ammonium sulfate approximately 31.83% of the activity was obtained in the fraction saturated with 80% ammonium sulfate. After ion-exchange chromatography two active β-glucosidase peaks were found (Figure 4.10). The major active peak was adsorbed onto the SP Seppharose Fast Flow column (fractions 53-66) and eluted from the column at 0.20-0.25 M NaCl, whereas the minor active peak (fractions 10-18) was not adsorbed on the resin and eluted with most of the loading protein in the wash with the starting buffer. The presence of multiple forms of β-glucosidase appears common among cellulolytic fungi and other microorganisms (Chen *et al.*, 1992; Chen *et al.*, 1994; and Shewale, 1982). In some cases, these have been shown to be true isoforms in the sense that they represent the products of separate genes. Several fungi have been reported to possess more than one gene encoding for proteins with β-glucosidase activity (Warren, 1998). The major active fractions were pooled, $(NH_4)_2SO_4$

was added to 30% final concentration, and the mixture was injected onto a Phenyl Sepharose column. The active peaks (fractions 37-48) were collected (Figure 4.11). Most proteins did not bind to the hydrophobic exchanger; while the enzyme was strongly adsorbed. The concentrated enzyme was then loaded on the Superdex 200 HR column (Figure 4.12). During gel filtration, one peaks of β-glucosidase activity (fractions 32) was eluted. The β-glucosidase was purified 50.23 fold to homogeneity with an overall enzyme yield of 6.28% and a specific activity of 77.86 U/mg of protein (Table 4.3). The specific activities of purified β-glucosidases from various microorganisms examined by other researchers varied from 5 to 979 U/mg of protein (Bronnenmeier and Staudenbauer, 1988; Freer, 1995; Kwon *et al.*, 1992; Li and Calza, 1991; and Watanabe *et al.*, 1992).

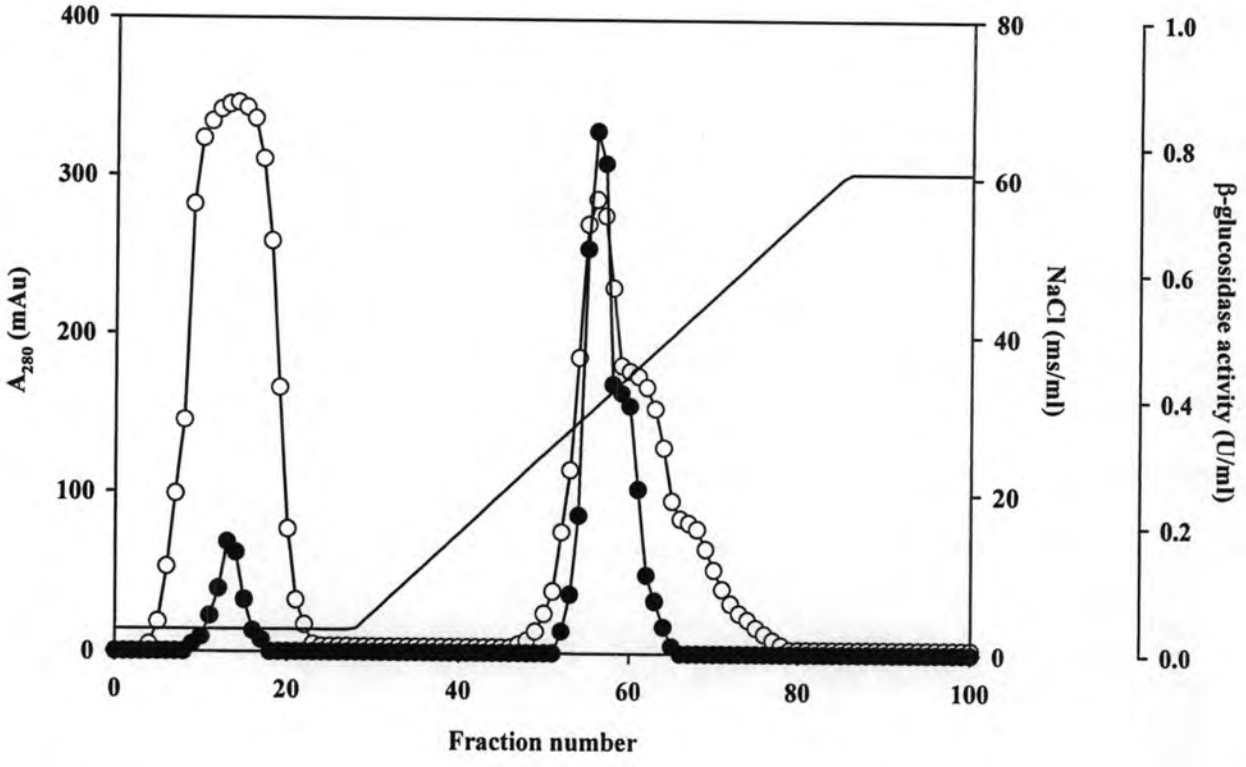

Figure 4.10 Purification of β-glucosidase from *D. eschscholzii* by SP Sepharose Fast Flow column

The enzyme solution was applied to SP Sepharose Fast Flow column (1.6 × 10 cm) and washed with 20 mM sodium acetate buffer, pH 5.0 until A_{280} decreased to base line. Elution of bound proteins was made by 0-1.0 M NaCl in the same buffer at the flow rate of 1.0 ml/min. The fractions of 10 ml were collected. The protein peaks from fraction number 53-66 were pooled.

(○) Absorbance at 280 nm (●) β-glucosidase activity (U/ml) (—) NaCl (ms/ml)

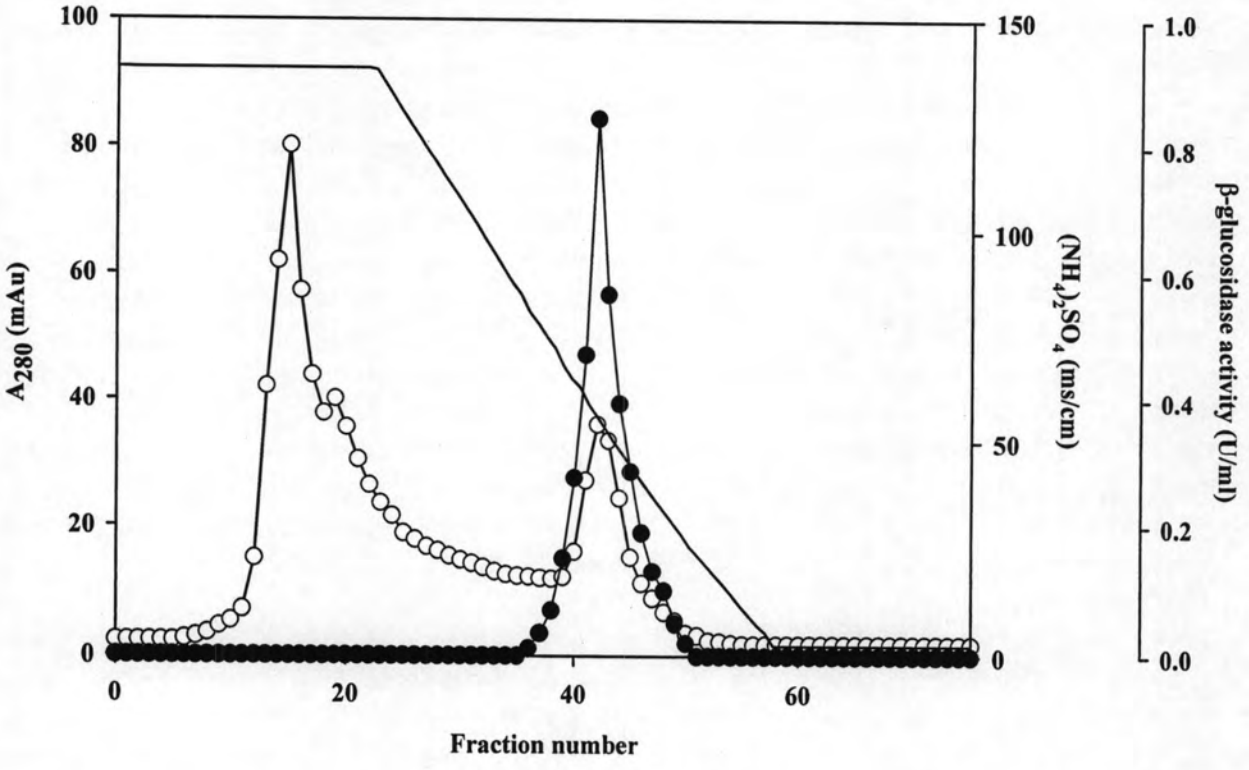

Figure 4.11 Purification of β-glucosidase from *D. eschscholzii* by Phenyl Sepharose Fast Flow column

The enzyme solution was applied to Phenyl Sepharose Fast Flow column (1.6 × 10 cm) and washed with 30% saturation with ammonium sulfate in 20 mM sodium acetate buffer, pH 5.0 until A_{280} decreased to base line. Elution of bound proteins was made by eluted 30-0% saturation ammonium sulfate in the same buffer. The fractions of 10 ml were collected. The protein peaks from fraction number 37-48 were pooled.

(○) Absorbance at 280 nm (●) β-glucosidase activity (U/ml) (—) $(NH_4)_2SO_4$ (ms/cm)

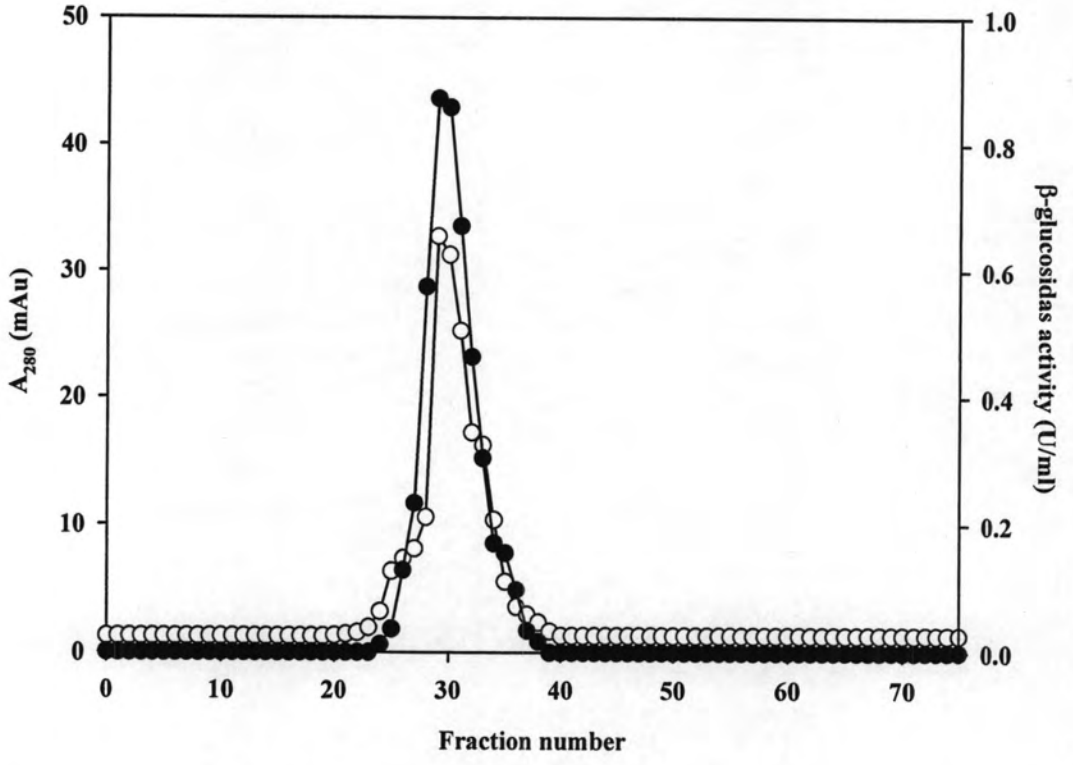

Figure 4.12 Purification of β-glucosidase from *D. eschscholzii* by Superdex-200 High Resolution column

The enzyme solution was applied to Superdex-200 High resolution column (1.6 × 60 cm) and equilibrated 100 mM in 20 mM sodium acetate buffer, pH 5.0 until A_{280} decreased to base line. Elution of bound proteins was made by eluted in the same buffer. The fractions of 5 ml were collected. The protein peaks from fraction number 29-30 were pooled.

(○) Absorbance at 280 nm (●) β-glucosidase activity (U/ml)

Table 4.4 Purification table of β-glucosidase from *D. eschscholzii*

Purification step	Total protein (mg)	Total activity (U)	Specific activity (U/mg)	Yield (%)	Purification (Fold)
Culture filtrate	695.47	1,078.96	1.55	100.00	1.00
$(NH_4)_2SO_4$ Precipitation	41.63	343.42	8.25	31.38	5.32
SP Sepharose Fast Flow (ion exchange)	3.75	175.61	46.83	16.28	36.21
Phenyl Sepharose Fast Flow (hydrophobic interaction)	1.42	98.53	64.72	9.13	41.75
Sephacryl S-100 HR	0.87	67.74	77.86	6.28	50.23

4.5.2 Determination of enzyme purity and protein pattern on native-PAGE

The enzyme from each step of purification was analyzed for purity and protein pattern by native-PAGE. The activity staining was performed to compare with protein staining. The result is shown in Figure 4.13. The enzyme in lane 4 showed a single protein band on native-PAGE. On the same gel, after staining for β-glucosidase activity using 4-methyllumberiferryl-β-glucoside, a single band visualized under UV light was observed at the same migration distance, indicating that the purified β-glucosidase from Superdex 200 HR Fast Flow column should be pure enzyme.

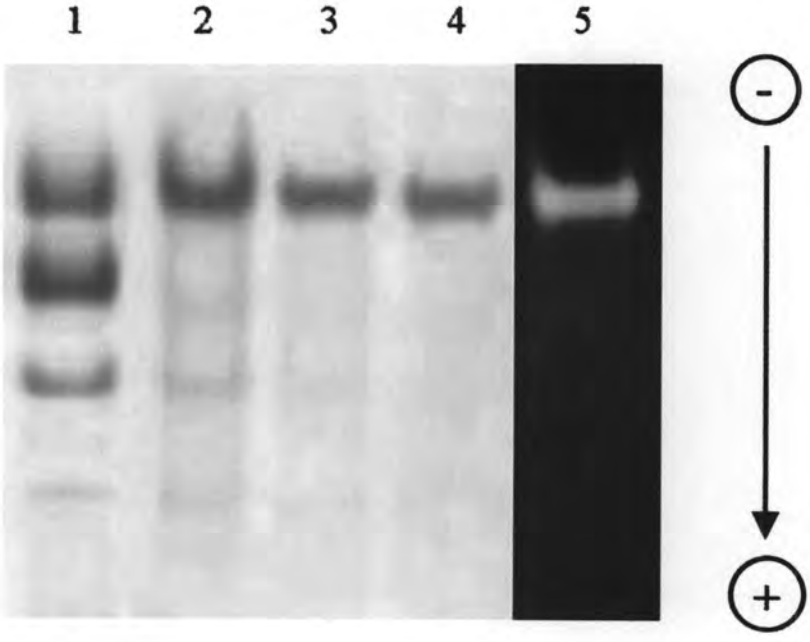

Figure 4.13 Non-denaturing PAGE of the *D. eschscholzii* β-glucosidase from each step of purification

Lane 1	Ammonium sulfate precipitation	50 μg of protein
Lane 2	SP Sepharose Fast Flow column	25 μg of protein
Lane 3	Phenyl Sepharose Fast Flow column	15 μg of protein
Lane 4	Superdex 200 HR Fast Flow column	15 μg of protein
Lane 5	Activity staining using 4-methyllumberiferryl-β-glucoside	10 μg of protein

4.6 Biochemical characterization β-glucosidase from *D. eschscholzii*

4.6.1 Molecular weight determination

SDS-PAGE analysis of the purified β-glucosidase showed the presence of a single band when stained with coomassie blue R-250 and it was about 64.2 kDa (Figure 4.14, 4.15).The molecular weight of the native β-glucosidase confirmed by MALDI-TOF mass spectrometer (Figure 4.16), the m/z of 65,747 Da was singlet charged species and m/z of 32,972 Da was doublet charged species of the same protein. The value was approximately 2.4 % more than the value obtained from SDS-PAGE, suggesting the enzyme is a monomer. The molecular mass of β-glucosidases from aerobic fungi ranges from 40 to 480 kDa (Dekker, 1981; and Wood and McCrae, 1982). The enzymes exhibiting subunit molecular mass in the range 40 to 60 kDa are generally monomeric whereas large subunit enzymes (80 to 100 kDa) are observed to be multimeric which could lead to their organization into multi-domain structures. A related category of enzymes, namely glycosyl transferases (responsible for glycosylation of proteins), are also large multimeric proteins organized into various domains (Saxena *et al.*, 1995) and it is not known whether β-glucosidases share significant sequence similarity with these enzymes.

4.6.2 Determination of isoelectric point

Analytical IEF data demonstrated that β-glucosidase from *D. eschscholzii* is an alkaline protein; it was isoelectric at pH 8.55 (Figure 4.17, 4.18). β-glucosidases from aerobic fungi generally have acidic *pIs* (Coughlan, 1985). However, β-glucosidases with basic *pIs* have also been reported, e.g. *Trichoderma reesei* (Schmid and Wandrey, 1987; Hofer *et al.*, 1989; and Chirico and Brown, 1987).

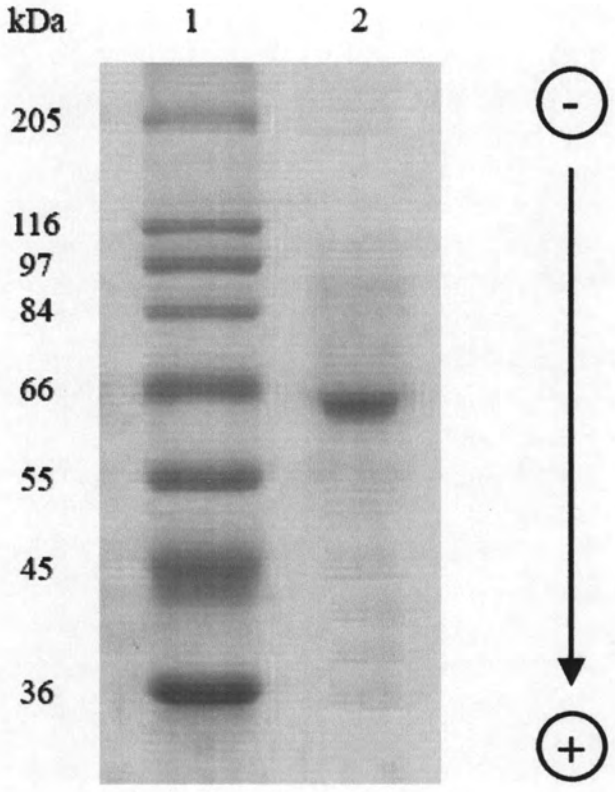

Figure 4.14 SDS-PAGE of purified β-glucosidase from *D. eschscholzii*

Lane 1	Molecular weight marker of protein standard	
	Myosin	205 kDa
	β-Galactosidase	116 kDa
	Phosphorylase b	97 kDa
	Fructose-6-phosphate kinase	84 kDa
	Albumin	66 kDa
	Glutamic dehydrogenase	55 kDa
	Ovalbumin	45 kDa
	Glyceraldehydes-3-phosphate dehydrogenase	36 kDa
Lane 2	Purified β-glucosidase	10 μg of protein

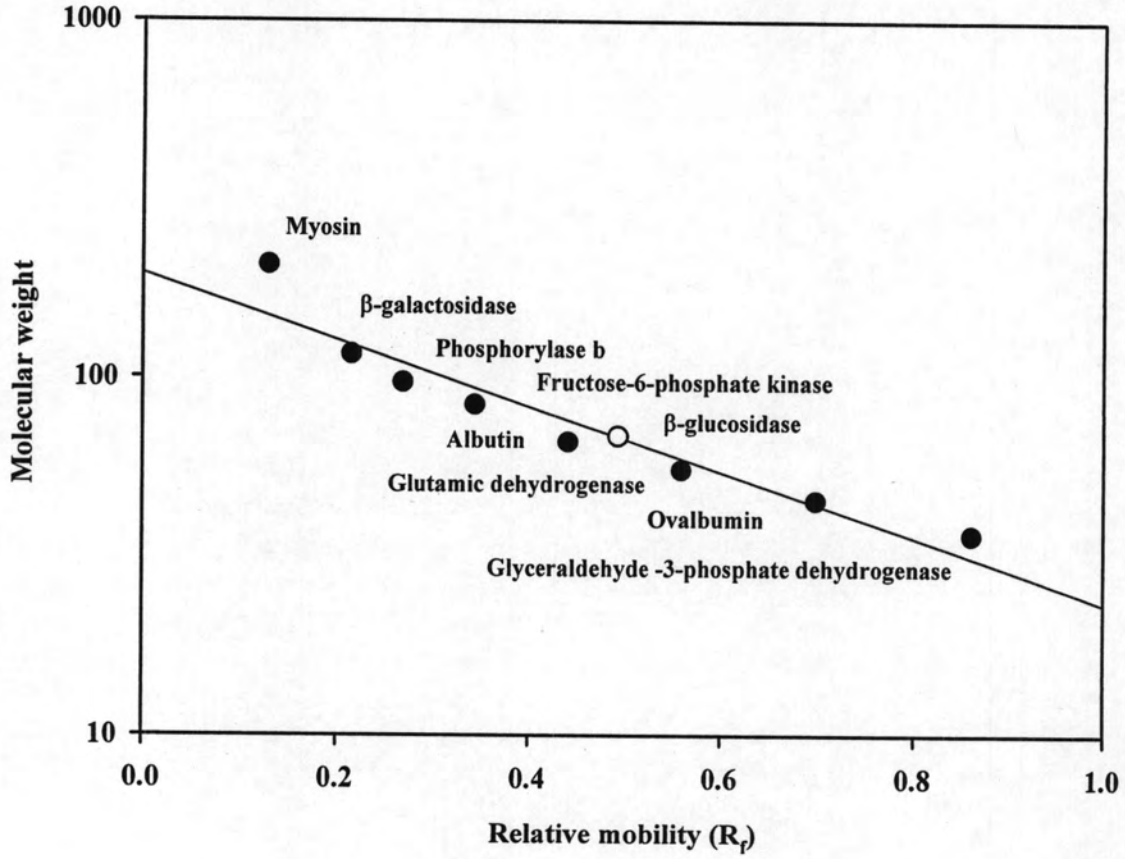

Figure 4.15 Standard curve of molecular weight and relative mobility of purified β-glucosidase from *D. eschscholzii* on SDS-PAGE

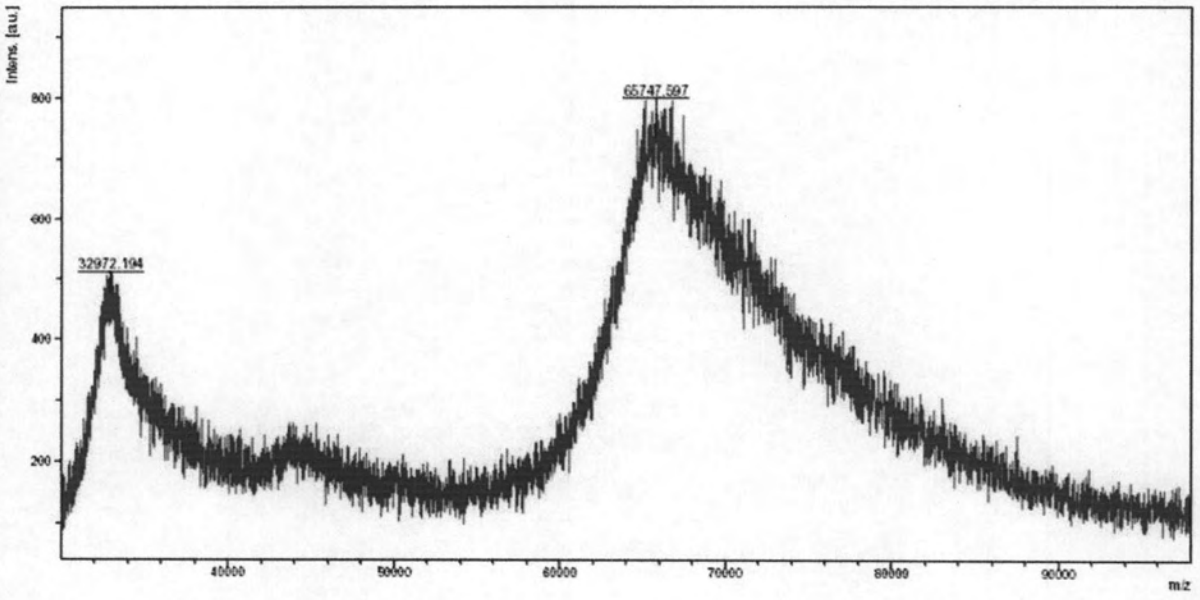

Figure 4.16 MALDI-TOF mass spectrum of purified β-glucosidase from Superdex-200 High Resolution column

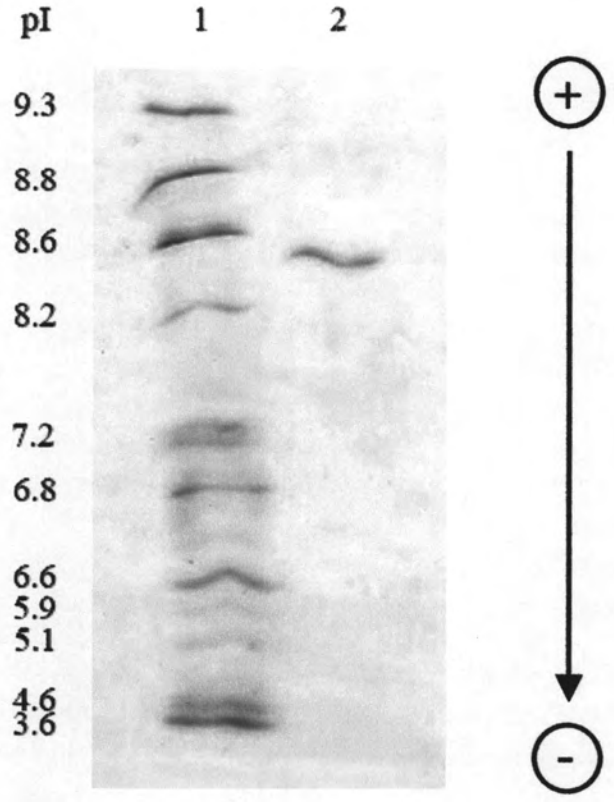

Figure 4.17 IEF-PAGE of purified β-glucosidase from *D. eschscholzii*

Lane 1	Standard pI markers	
	Amyloglucosidase	(pI 3.6)
	Trypsin inhibitor	(pI 4.6)
	β-Lactoglobulin A	(pI 5.1)
	Carbonic anhydrase II	(pI 5.9)
	Carbonic anhydrase I	(pI 6.6)
	Myoglobin acidic band	(pI 6.8)
	Myoglobin basidic band	(pI 7.2)
	Lentil lectin acidic band	(pI 8.2)
	Lentil lectin middle band	(pI 8.6)
	Lentil lectin basic band	(pI 8.8)
	Trypsinogen	(pI 9.3)
Lane 2	Purified β-glucosidase	5 μg of protein

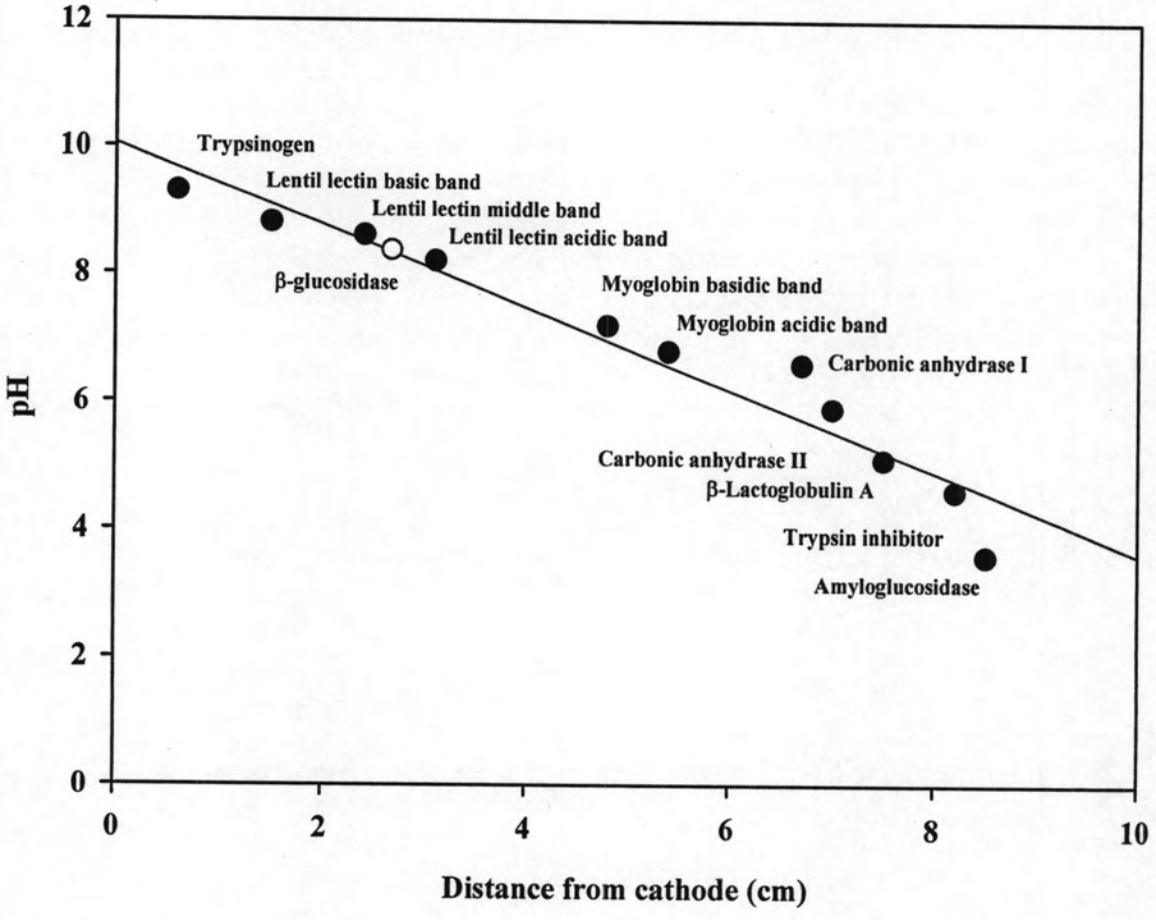

Figure 4.18 Standard curve of *pI* determination

4.6.3 Effect of temperature on β-glucosidase activity and stability

The purified β-glucosidase activity was measured at temperatures ranging from to 30 °C to 80 °C. Optimum activity was observed at 50 °C, however, the enzyme retained only 8.46% of its maximal activity when the temperature was increased to 60 °C. Similar temperature optima of β-glucosidases ranged from 50 to 65 °C have been reported from several fungi, such as *Aspergillus niger* (Yan and Lin, 1997), *Aspergillus tubingensis* (Decker *et al.*, 2001), *Fusarium oxysporum* (Christakopoulos *et al.*, 1994), and *Neurospora crassa* (Yazdi *et al.*, 2003). Thermostability tests showed that the enzyme appeared to be stable and retained its full activity after 30 min incubation at 50 °C and retained about 73.55% activity at 50 °C. β-Glucosidase activity decreased dramatically when the incubation temperature increased above 50 °C, and very little activity was observed after 30 min incubation at 70 °C (Figure 4.19).

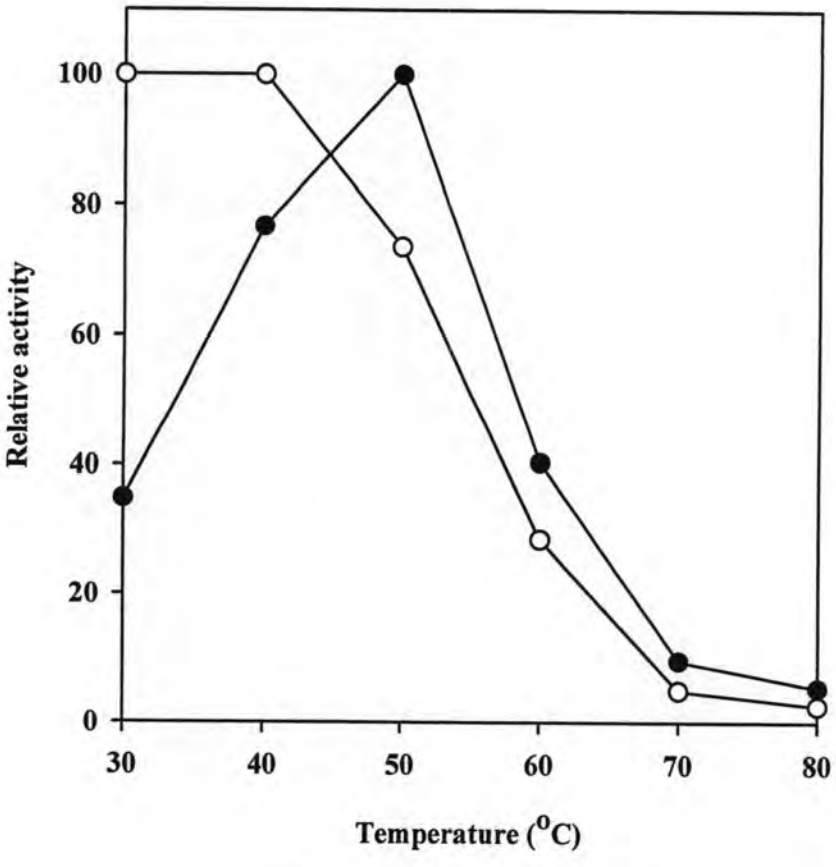

Figure 4.19 Temperature activity (●); and temperature stability (○). The following buffer systems were used 0.1 M acetate pH 5.5. The values shown represent averages from triplicate experiments.

4.6.4 Effect of pH on β-glucosidase activity and stability

The optimum pH for purified β-glucosidase activity was explored. The highest activities occurred at pH 5.0 and decreased rapidly after pH 7.0, and are similar above to that reported for β-glucosidase from *Aspergillus* species (Riou *et al.*, 1998; Yan and Lin, 1997). The enzyme was stable at pH 5.0 to 8.0 for at least 1 h at 30 °C, with 62.49% activity remaining at pH 4.0 and 79.46% activity remaining at pH 9.0. The enzyme was fairly stable in the pH rage of pH 5.0 to 8.0, retaining over 85% activity. The enzyme, however, was shown to be sensitive to pH below 4.0 since it lost its activity at pH 3.0. Conversely, it was found very stable under neutral and alkaline pH since it retained up to 75% of its activity at pH 9.0 (Figure 4.20). Most fungal β-glucosidases exhibit pH optima ranging from 5.0 to 6.5 (Bhatia *et al.*, 2002).

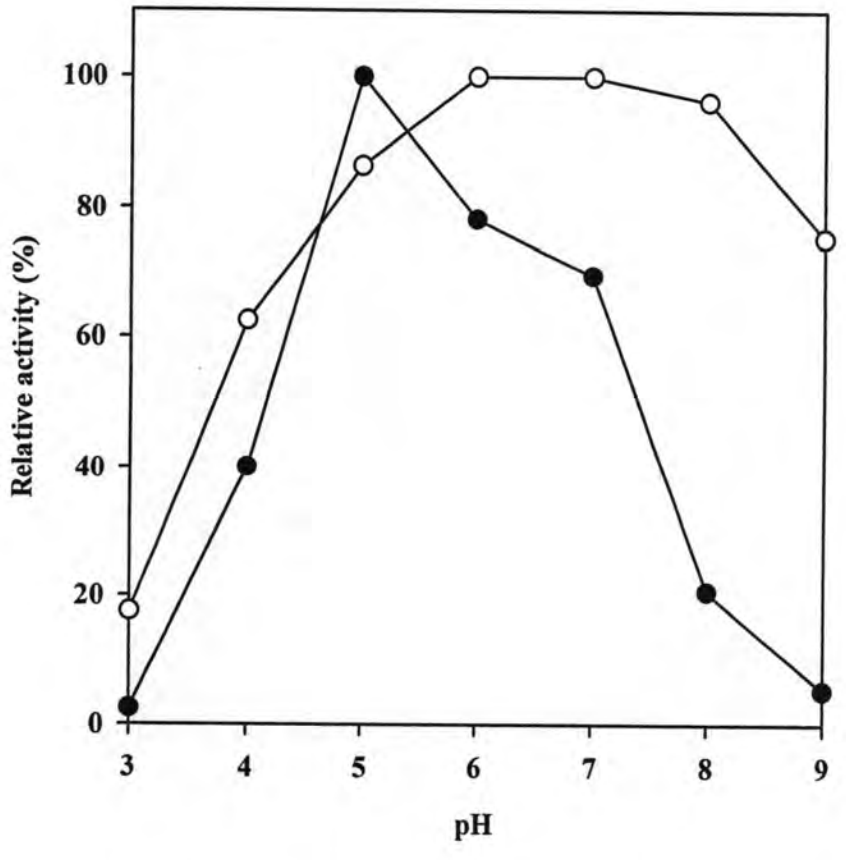

Figure 4.20 pH activity (●); and pH stability (○). The following buffer systems were used: 0.1 M sodium acetate buffer (pH 3.0-6.0); 0.1 M phosphate buffer (pH 6.0-7.0) and Tris-HCl buffer (pH 7.0-9.0). The values shown represent averages from triplicate experiments.

4.6.5 Effect of metals and reagents

The enzyme activity was strongly inhibited by the sulfhydryl oxidant which have been generally reported as a strong inhibitor for fungal β-glucosidases (Li and Calza, 1991; Cao and Crawford, 1993; Gueguen *et al.*, 1995; and Sasaki and Nagayama, 1995), but we observed that some metal ions activate the enzyme (Table 4.4). This result suggested that the thiol group was essential for β-glucosidase activity (Inglin *et al.*, 1980). This was further confirmed by the observation that Hg^{2+} ions completely inactivated the enzyme. The role of -SH groups in activity of β-glucosidases has been observed in some microbial β-glucosidases (Marchin and Duerksen, 1969; and Li and Calza, 1991). The chelating agent EDTA did not affect β-glucosidase activity, indicating that β-glucosidase is not a metalloprotein. Comparably, DTT is not an inhibitor, suggesting that disulfide bonds are not essential for the enzyme activity. Activation by Ca^{2+}, Co^{2+}, Mn^{2+}, Mg^{2+}, glycerol and DMSO may be explained by the stabilization of the enzyme structure.

Table 4.4 Effect of some cations and other reagents on purified β-glucosidase activity from *D. eschscholzii*

Reagent[a]	Relative activity (%)[b]
Control[c]	100.0
$CaCl_2$	107.3
$CoCl_2$	101.6
$CuSO_4$	85.2
$HgCl_2$	6.8
$FeCl_2$	78.7
$MgSO_4$	122.3
$MnCl_2$	118.5
$ZnSO_4$	92.0
DMSO[d]	102.8
DTT[e]	107.5
EDTA[f]	108.3
Glycerol	104.6

[a]The assays were carried out in the presence of 1 mM concentrations of each of the metal ions and reagents.

[b]The relative activity was determined by measuring β-glucosidase at 50 °C in 0.1 M sodium acetate buffer pH 5.0 after pre-incubation at 30 °C for 30 min with individual cations or reagents. Results are shown as the average p-nitrophenol released from a representative assay performed in triplicate.

[c]The activity assayed in the absence of cations or reagents was taken as 100%.

[d]DMSO; dimethyl sulfoxide

[e]DTT; dithiothreitol

[f]EDTA; ethylenediaminetetraacetic acid

4.6.6 Substrate specificity

β-Glucosidase may be divided into three groups on the basis of substrate specificity: (*i*) aryl-β-glucosidases, which have a strong affinity for aryl-β-glucosides; (*ii*) cellobiases, which hydrolyze only oligosaccharides; and (*iii*) broad-specificity β-glucosidases, which exhibit activity on many substrate types and are the most commonly observed β-glucosidase (Rojas *et al.*, 1995). The purified β-glucosidase from *D. eschscholzii* is a broad-specificity type, since it can hydrolyze a range of (β-1, 2), (β-1, 3), (β-1, 4), and (β-1, 6) diglycosides, as well as saccharides and aryl-β-glycosides. The purified enzyme had none or very little (≤8.5%) activity on lactose, maltose, sucrose, Avicel, and carboxymethyl cellulose. It had very little (≤7.0%) activity on p-nitrophenyl-β-D-xylopyranoside and o-nitrophenyl-β-D-galactopyranoside. o-Nitrophenyl-β-D-glucopyranoside was hydrolyzed at 15.5% of the level of hydrolysis of PNPG (Table 4.5). β-Glucosidases with very broad specificity have been isolated from many fungi (Copa-Patino and Broda 1994; Gueguen *et al.*, 1995; Kwon *et al.*, 1992; Pitson *et al.*, 1997; Watanabe et al 1992; Wood and McCrae 1982).The results of previous studies suggest, however, that many broad-specificity enzymes that exhibit exo-β-(1,3)- and exo-β-(1,6)-glucanase activities with glucose as the only product of hydrolysis are β-glucosidases rather than exo-β-glucanases (Copa-Patino and Broda, 1994; Fontaine *et al.*, 1997; Pitson *et al.*, 1993; Pitson *et al.*, 1997; and Rapp, 1989).

Table 4.5 Substrate specificity by purified endoglucanase activity from *D. eschscholzii*

Substrate	Relative activity (%)[a]
Saccharides	
cellobiose (20 mM) (β-1, 4) Glc	100.0
sophorose (20 mM) (β-1, 2) Glc	79.5
laminaribiose (20 mM) (β-1, 3) Glc	65.7
gentiobiose (20 mM) (β-1, 6) Glc	76.8
lactose (20 mM) (β-1, 4) Gal	2.5
maltose (20 mM) (α-1, 4) Glc	6.2
sucrose (20 mM) fructose (1, 2) Glc	0.0
Avicel® PH 101 (1%, wt/vol)	0.0
carboxymethyl cellulose (CMC; 1%, wt/vol)	8.5
Aryl-glycosides	
p-nitrophenyl-β-D-glucopyranoside (5 mM)	100.0
o-nitrophenyl-β-D-glucopyranoside (5 mM)	11.5
p-nitrophenyl-β-D-xylopyranoside (5 mM)	7.5
o-nitrophenyl-β-D-galactopyranoside (5 mM)	0.0

[a]Values shown are the averages from triplicate experiments with each substrate. Activity of the saccharides was determined by measuring the release of glucose (DNS method), and on aryl-glucosides by measuring the release of PNPG. Sufficient enzyme was used to ensure a linear release of product during the first 10 min of reaction at 0.1 M sodium acetate buffer pH 5.0 and 50 °C. The relative initial rate of hydrolysis of a saccharide is expressed as a percentage of that obtained with cellobiose and that of an aryl-glucoside is expressed as a percentage of that obtained with PNPG.

4.6.7 Effect of alcohols

The inclusion of increasing amount of alcohols had varying effects on the activity with the substrate PNPG (Figure 4.21). Methanol, ethanol, *n*-propanol, and *n*-butanol resulted in a decrease of β-glucosidase activity as the concentration of alcohol increased. This effect was more pronounced as the length of the alcohol chain increased. At the higher concentrations, the enzyme was inhibited by ethanol probably because of protein denaturation. The effect of *n*-propanol, and *n*-butanol on activity was biphasic with activity increased at low concentrations and decreased at high concentrations. It was not possible to analyze effects of long-chain alcohols at the higher concentrations than those tested, because of their limited solubility in aqueous solutions. The effect of increasing β-glucosidase activity in the presence of alcohols is believed to occur because alcohols are generally stronger nucleophiles than water in reactions involving nucleophilic substitutions (Sinnot, 1990; and Withers and Street, 1989). However, it is not only the hydrophobicity, but also the length of the alkyl chain and the shape of the molecule that appeared to be critical determination in this interaction (Glew *et al.*, 1993) as confirmed by these results. Activation by alcohols have been observed for β-glucosidases from *Aspergillus niger* (Yan and Lin, 1997; Watanabe *et al.*, 1992), *Botrytis cinerea* (Gueguen *et al.*, 1995), *Candida peltata* (Saha and Bothast, 1996), *Thermotoga* sp. (Ruttersmith and Daniel, 1993), and *Fusarium. oxysporum* (Christakopoulos *et al.*, 1994).

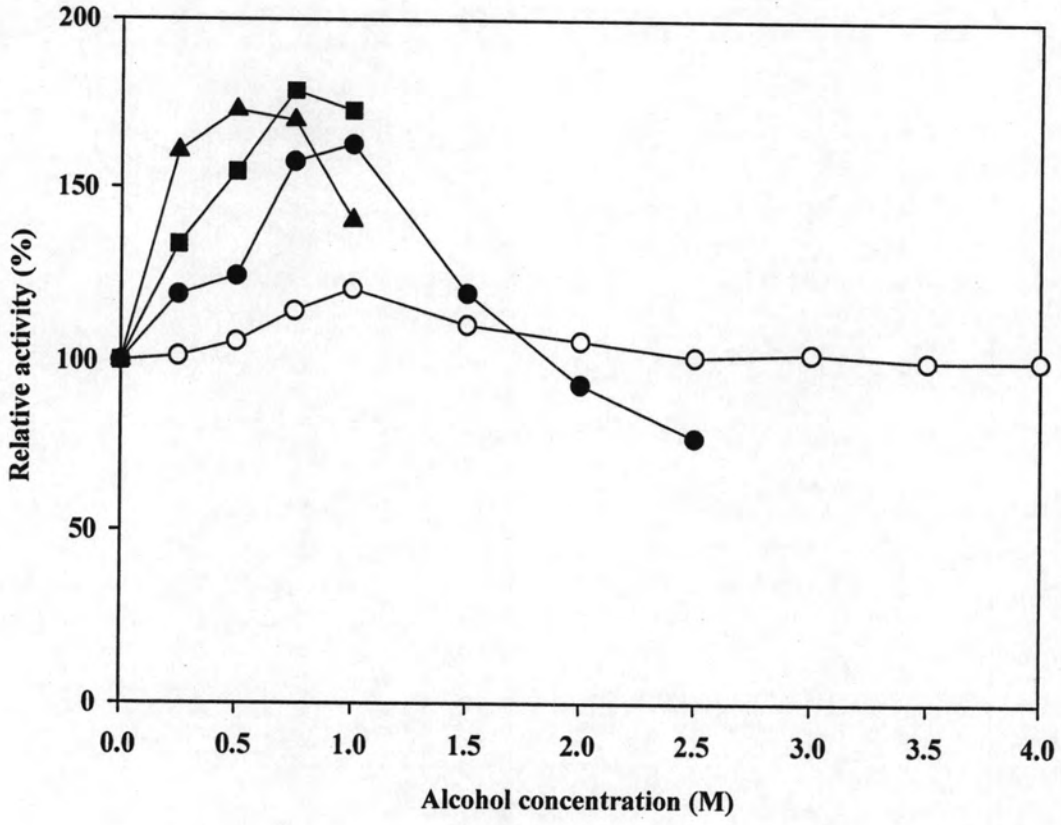

Figure 4.21 Effect of *n*-alcohols on activity of the purified β-glucosidase. Addition of *n*-alcohol: (○) methanol; (●) ethanol; (■) *n*-propanol; and (▲) *n*-butanol. The concentration of *n*-propanol, and *n*-butanol are less than 1.0 M because of limited solubility in aqueous solution

4.7 Kinetic mechanism studies of β-glucosidase from *D. eschscholzii*

4.7.1 Determination of kinetic constant

Reaction kinetics of the purified β-glucosidase was determined from Lineweaver-Burk plots with PNPG as substrate under defined assay conditions. The enzyme had K_m a value of 1.52 mM, and a V_{max}, value of 3.21 U/min/mg of protein (Figure 4.22). In the case of β-glucosidase from *D. eschscholzii*, the K_m values for PNPG is similar to the fungal β-glucosidase from literature data such as *Aspergillus fumigatus* (Kitpreechavanich *et al.*, 1986), *Aspergillus wentii* (Srivastava *et al.*, 1984), and *Sclerotium rolfsii* (Sadana *et al.*, 1988) with K_m values of 1.4, 1.6, and 1.38 mM respectively.

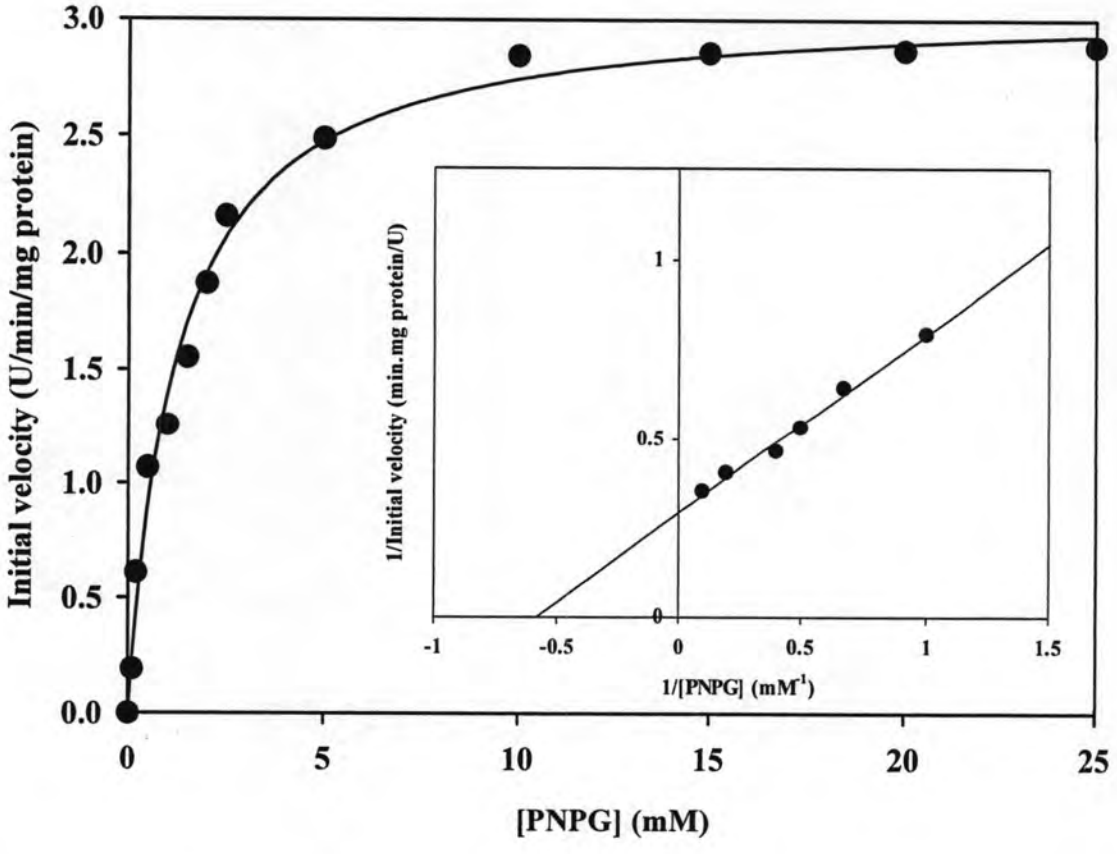

Figure 4.22 Variation of initial velocity with PNPG concentration in the hydrolysis reaction of purified β-glucosidase. K_m and V_{max} were 1.52 mM, and 3.21 U/min/mg of protein, respectively

4.7.2 Inhibitory effect of glucose and glucono-δ-lactone

Glucose was found to be a competitive inhibitor of the enzyme as shown by a Lineweaver-Burk plot in the presence of various concentrations of glucose. As the glucose concentration increased the apparent K_m for the PNPG decreased, whereas the maximum velocity remained the same. The inhibitory effect of glucose reveals that the interaction with the carbohydrate moiety of the substrate is as important as with the hydrophobic aglycone. The K_i was found to be 0.79 mM for glucose when PNPG was used as the substrate (Figure 4.23). Competitive inhibition by glucose is a common characteristic of fungal β-glucosidases although there are exceptions like β-glucosidases produced by several *Aspergillus* species (Riou *et al.*, 1998; Decker *et al.*, 2001; and Yan and Lin, 1997). Most microbial β-glucosidases have glucose inhibition constants ranging from 0.35 mM to no more than 100 mM (Riou *et al.*, 1998). The glucose inhibition constant for this β-glucosidase is one of the smallest values reported for fungal β-glucosidases (Christakopoulos *et al.*, 1994; Lo *et al.*, 1990; Guegen *et al.*, 1995; and Saha *et al.*, 1996).

Glucono-δ-lactone, which is known to be structural similarity with an intermediary compound of the reaction, was by far the most potent inhibitor for this β-glucosidase, a characteristic common to other fungal β-glucosidases. The K_i was found to be 4.72 μM for glucono-δ-lactone when PNPG was used as the substrate (Figure 4.24). The strong inhibitory effect of glucono-δ-lactone proves that in the transition state the substrate is distorted into half chair conformation. K_i values reported for glucono-δ-lactone are in the range of 4-20 μM (Pitson *et al.*, 1997; Christakopoulos *et al.*, 1994; Lo *et al.*, 1990; Guegen *et al.*, 1995). The comparison of the K_i values for the purified β-glucosidase indicated that glucono-δ-lactone inhibited 1.67×10^{-4} times more strongly than glucose. Although the above values are quite close for purified β-glucosidase from *D. eschscholzii*, it indicated a possible higher resistance for this enzyme against both inhibitors.

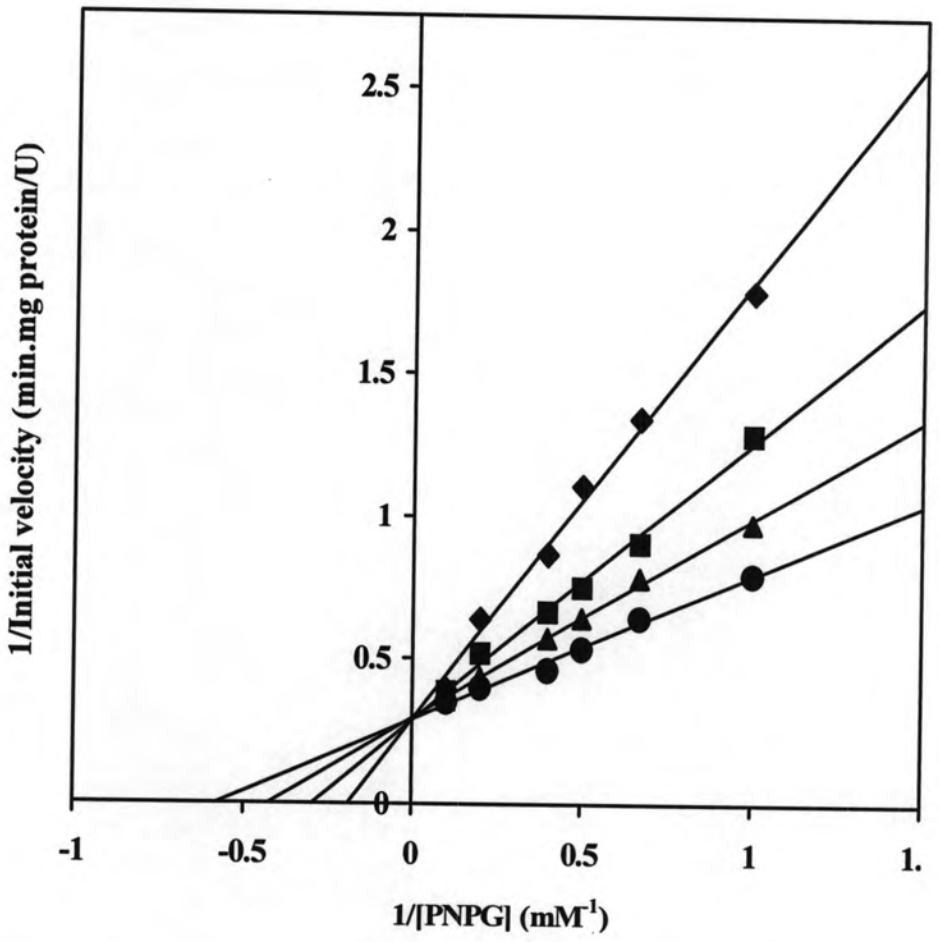

Figure 4.23 Lineweaver-Burk plot of PNPG hydrolysis by purified β-glucosidase in the presence of glucose. Addition of glucose: (●) 0 mM; (▲) 2.5 mM; (■) 5.0 mM; and (♦) 10 mM. The intersection with the abscissa yielded a K_i and was found to be 0.79 mM

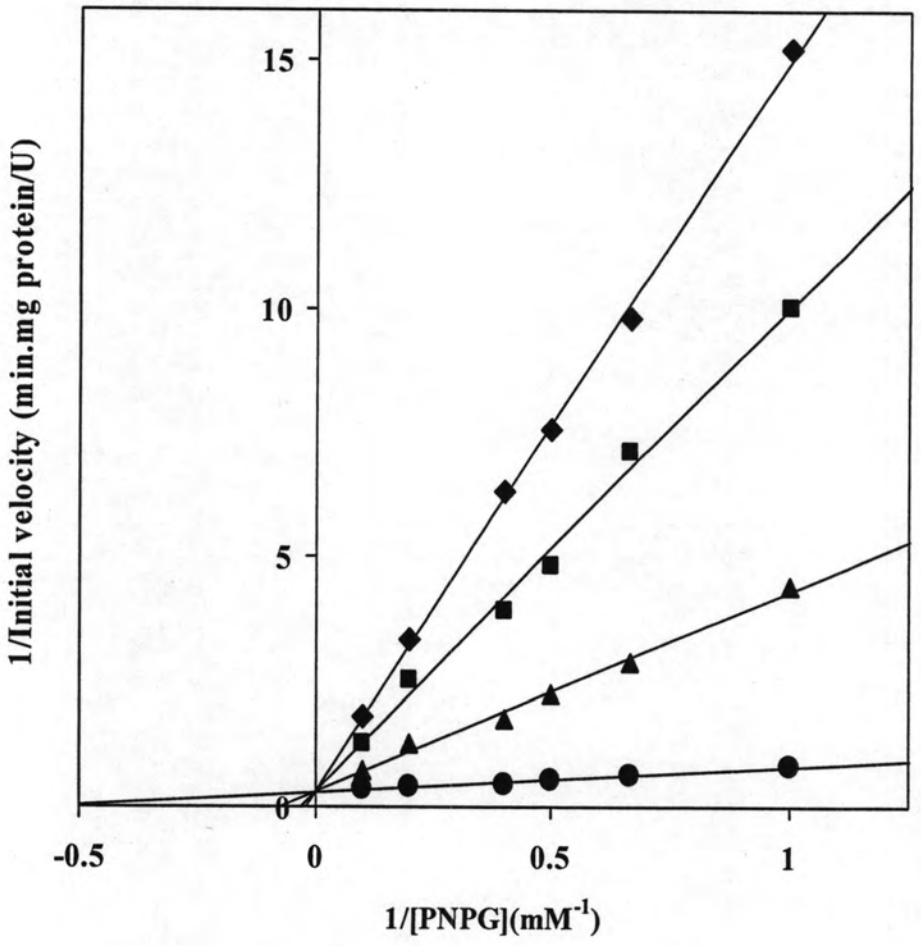

Figure 4.24 Lineweaver-Burk plot of PNPG hydrolysis by purified β-glucosidase in the presence of glucono-δ-lactone. Addition of glucono-δ-lactone: (●) 0 mM; (▲) 1.25 mM; (■) 2.5 mM; and (♦) 5 mM. The intersection with the abscissa yielded a K_i and was found to be 4.72 μM

4.7.3 Identification of active-site residues by carboxyl group modification

The modification by EDC requires that the carboxyl groups be protonated or in un-ionized form. Semi-logarithmic plots of β-glucosidase as a function of time at different EDC concentrations in the presence of excess glycinamide as nucleophile were linear (Figure 4.25), identicating that the inactivation followed pseudo-first-order kinetics. The rate of the modification reaction is retarded in the presence of an added nucleophile (Chan *et al.*, 1988). The modification reaction was always performed in the presence of an added nucleophile, to avoid the introduction of a bulky group into the enzyme. These bulky groups could cause unwanted conformational changes and a disruption of structure, resulting in faster inhibition. Furthermore, the addition of a nucleophile helps to prevent the secondary modification of amino groups of the enzyme by consuming the activated carboxyl groups as a result of reaction quenching. The plot of apparent pseudo-first-order rate constants (k) against EDC concentration was also linear and gave a second-order rate constant of 6.73 × 10-2 mM/min (Figure 4.25, left inset). The log-log plot of pseudo-first-order rate constants (k) against EDC concentration (Figure 4.25, right inset) gave a slope of 1.14 suggesting that the reaction is first-order with respect to EDC, and one carbodi-imide molecule is needed to the inhibit one molecule of β-glucosidase.

To further determine if the amino acid residues are at the active site of β-glucosidase from *D. eschscholzii*, glucono-δ-lactone was included in the modification reaction. As a competitive inhibitor, glucono-δ-lactone should bind at the enzyme active site and prevent the modification of the amino acids at the active-site. In the presence of this inhibitor, the inactivation of the enzyme by the chemical modification should be prevented. When the inactivation of β-glucosidase by EDC was performed in the presence of glucono-δ-lactone, the pseudo-first-order rate constants decreased with increasing glucono-δ-lactone concentration (Figure 4.26). The secondary plot of protection against glucono-δ-lactone concentration (Figure 4.26, inset) gave a k_d of 70.74 × 10^{-2} mM for the enzyme-glucono-δ-lactone complex. Moreover, it showed that the protection of the active-site carboxy group by glucono-δ-lactone from EDC was only partial because the line did not pass through the origin. This signifies that the carboxyl group is essential for catalysis but not for substrate binding, as it is not fully protected by glucono-δ-lactone.

The technique of chemical modification has been used not only to identify the active-site residues but also to alter the kinetic properties of the enzyme (Lundblad, 1995). Previously, only two studies have been made of carboxyl group modification of fungal β-glucosidases from *Schizophyllum commune* (Clarke, 1990), and *Trichoderma reesei* (Mata *et al.*, 1990). These studies investigated the active-site residues; the enzyme was modified by EDC in the absence of an added nucleophile (Clarke, 1990).

The role of the conserved Asp residues in family 3 β-glucosidases was established following studies with BGL A3 of *Aspergillus wentii*, using a labeled inhibitor (conduritol B-epoxide) and trapping the enzyme-glycosyl intermediate with labeled 2-deoxy 2-fluoro β-glucosyl fluoride. On peptic cleavage and sequencing, the burst of radioactivity was found to be associated with the Asp residue (in conserved SDW motif) that served as the nucleophile. The peptide containing this signature motif was also found to be bound to the substrate by forming a covalent glucosyl intermediate (Bause and Legler, 1980). More recently, BGLI isolated from *Pichia etchellsii*, and belonging to family 3 of glycosylhydrolases, was found to contain a catalytically important Asp/Glu residue (Wallecha, 2001).

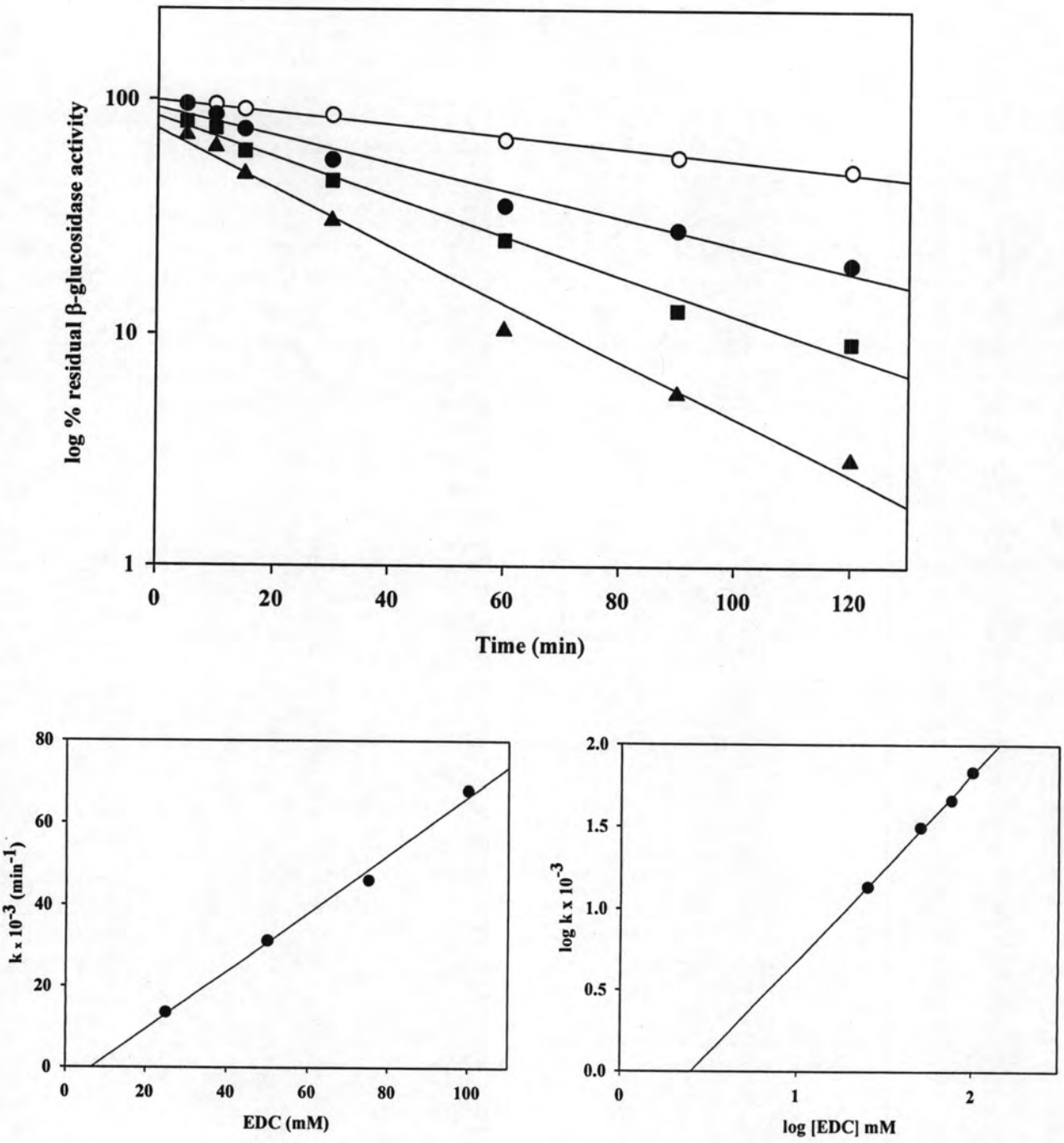

Figure 4.25 First-order plots for the inactivation of β-glucosidase by varying amounts of EDC in the presence of glycinamide. Final EDC concentrations were: (○) 25 mM; (●) 50 mM; (■) 75 mM; and (▲) 100 mM. Pseudo-first-order constant (k) = slope × 2.303. Left inset: secondary plot for the determination of second-order rate constant. Right inset: log-log plot of pseudo-first-order rate constants (k) against [EDC]. The slope gives the reaction with respect to EDC concentration

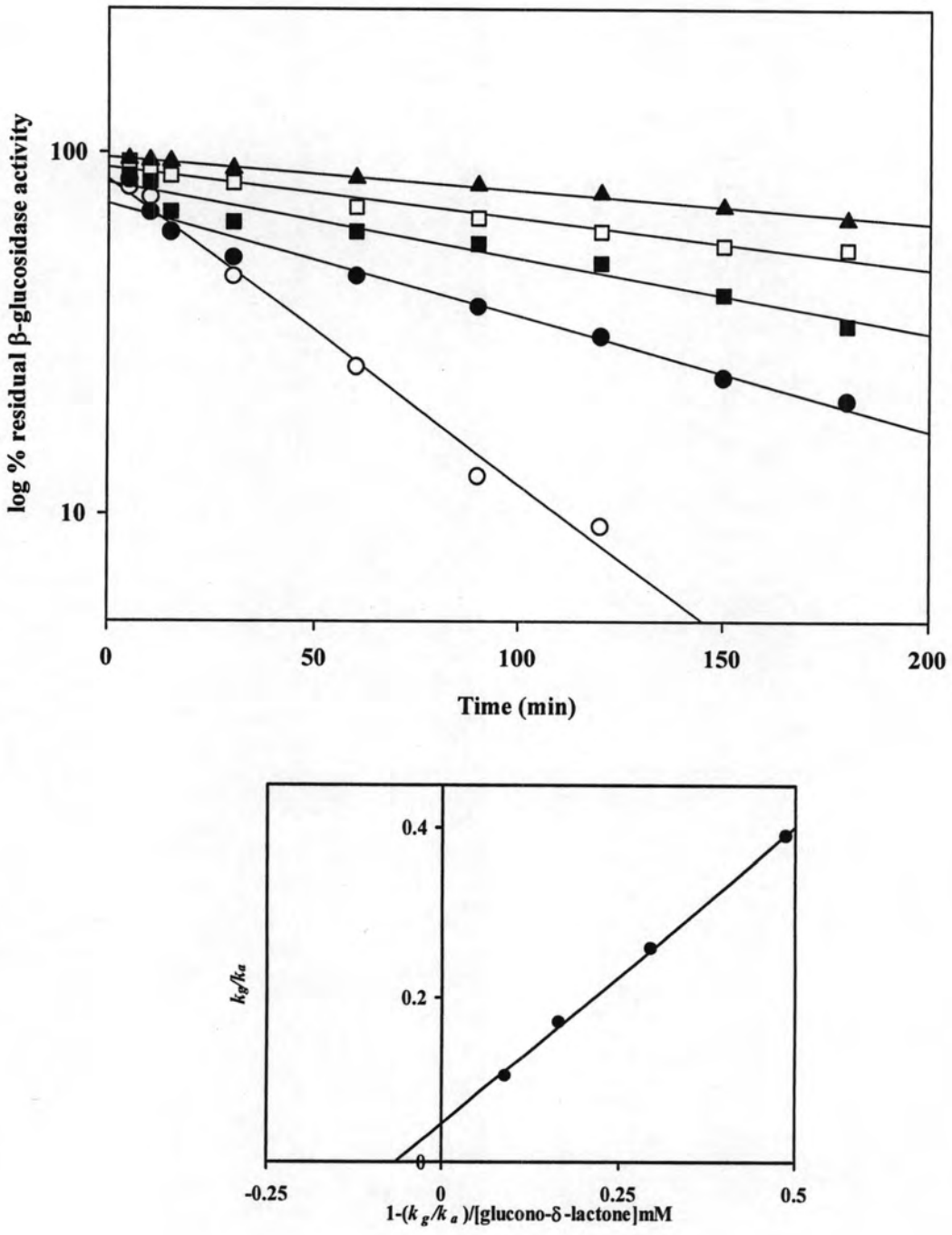

Figure 4.26 First-order plots for protection of β-glucosidase from EDC modification by variable concentrations of glucono-δ-lactone. Final glucono-δ-lactone concentrations were: (○) 0 mM; (●) 1.25 mM; (■) 2.5 mM; (□) 5 mM; 10 mM; and (▲) 100 mM. Pseudo-first-order constant (k) = slope×2.303. Inset: determination of k_d for enzyme- glucono-δ-lactone-complex. The apparent ratio of pseudo-first-order rate constants obtained in the absence (ka) and the presence (kg) of glucono-δ-lactone was ploted. The dissociation constant (k_d) = slope

4.8 Identification of β-glucosidase from *D. eschscholzii*

The internal sequence analysis of the purified β-glucosidase was obtained by digestion with trypsin and sequence analysis with LC-MS/MS and was found to be **TDGSNGDVASDWYHR** (Figure 4.27). Comparisons were then made to all protein sequences in the SwissProt database using the search protocol BLAST (Altschul *et al.*, 1990). Based on amino acid sequence similarities, glycosidases have been classified into several families, with most β-glucosidases belonging to either family 1 or family 3 (Henrissat *et al.*, 1995; Henrissat 1998) A high degree of internal amino acid sequence identity between *D. eschscholzii* β-glucosidase and other β-glucosidases of family 3 suggested that this enzyme could be a member of glycoside hydrolase family 3 (Figure 4.26). In addition, the active site of this enzyme contains several conserved residues, including a nucleophile (Asp) and an acid/base catalyst (Glu). Sequence alignment of the region containing the proposed catalytic nucleophile of over 15 β-glucosidases of family 3 shows the presence of Asp as a fully conserved catalytic nucleophile (Dan *et al.*, 2000). The data presented here shows that the β-glucosidase from *D. eschscholzii* follows a retention mechanism, and most probably belongs to family 3 of the glycoside hydrolase, as well as possessing an Asp or a Glu residue as a catalytic nucleophile.

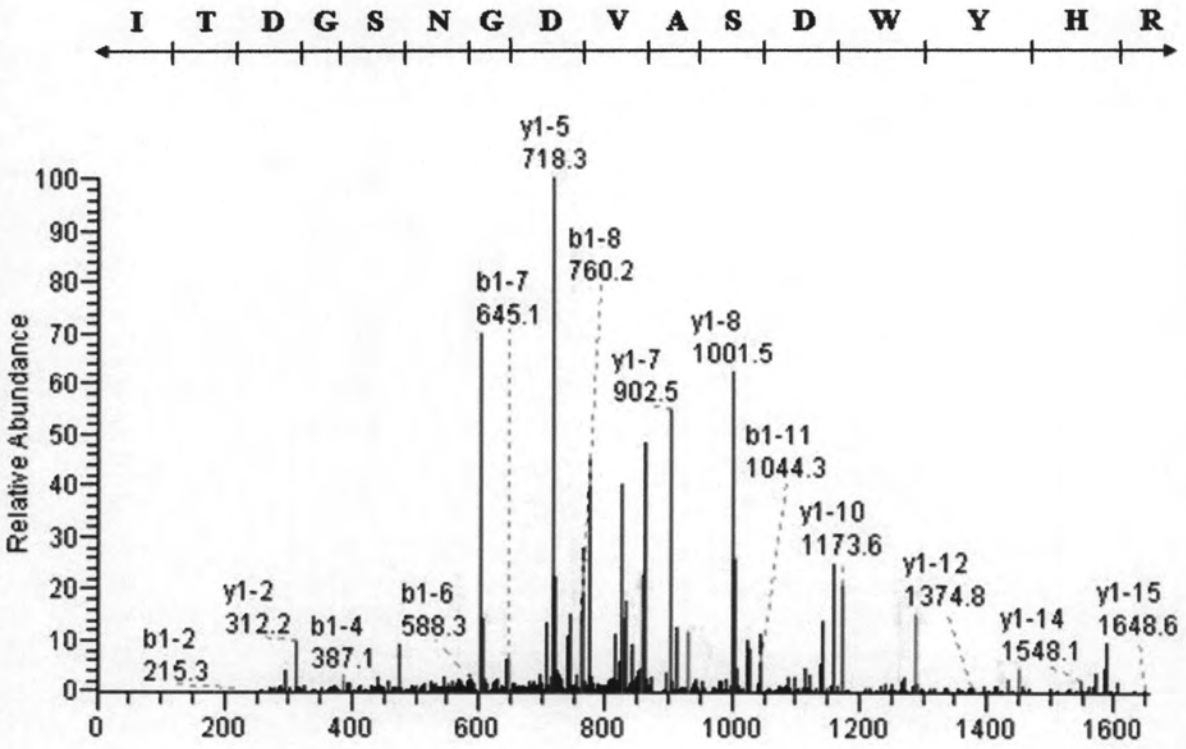

Figure 4.27 MS-MS spectra of purified β-glucosidase from *D. eschscholzii* tryptic peaks

																			Accession Number
Daldinia eschscholzii		**I**	**T**	**D**	**G**	**S**	**N**	**G**	**D**	**V**	**A**	**S**	**D**	**W**	**Y**	**H**	**R**		
Aspergillus fumigatus	**280**	**A**	**E**	**L**	**G**	**F**	**Q**	**G**	**F**	**V**	**M**	**S**	**D**	**W**	**S**	**A**	**H**	**295**	**Q4WJJ3**
Aspergillus niger	**269**	**A**	**E**	**L**	**G**	**F**	**Q**	**G**	**F**	**V**	**M**	**S**	**D**	**W**	**A**	**A**	**H**	**284**	**Q30BH9**
Fusarium graminearum	**284**		**E**	**M**	**G**	**F**	**Q**	**G**	**F**	**V**	**M**	**S**	**D**	**W**	**Q**	**A**	**Q**	**298**	**Q4I853**
Neurospora crassa	**283**		**E**	**N**	**G**	**F**	**Q**	**G**	**F**	**V**	**M**	**S**	**D**	**W**	**Q**	**A**	**H**	**297**	**Q7RWP2**
Phanerochaete chrysosporium	**52**			**D**	**G**	**K**	**N**	**G**	**D**	**V**	**A**	**T**	**D**	**S**	**Y**	**N**	**R**	**65**	**Q25BW4**
Talaromyces emersonii	**56**			**D**	**G**	**T**	**N**	**G**	**D**	**V**	**A**	**C**	**D**	**S**	**Y**	**H**	**R**	**69**	**Q8X214**
Trichoderma reesei	**48**			**N**	**G**	**A**	**N**	**G**	**D**	**V**	**A**	**C**	**D**	**H**	**Y**	**H**	**A**	**60**	**Q7Z9M2**

Figure 4.28 Amino acid sequences from the fragment obtained by tryptic digestion of the purified β-glucosidase from *D. eschscholzii*. Comparisons are made with other β-glucosidases classified as family 3 glucosyl hydrolases.

4.9 Synthesis of alkyl-glucosides using β-glucosidase

4.9.1 Alkyl-glucosides synthesis using transglycosylation

The synthesis of various alkyl-glucosides, such as primary, secondary and tertiary glusosides, was performed using purified β-glucosidase from *D. eschscholzii*. The reaction mixture resulted in separation of the pure products, which were identified by TLC. As observed, respective alkyl-glucosides, identified by comparision with the standard of glucose, cellobiose, and PNPG (Figure 4.29). All of the products were confirmed by ^{1}H NMR spectrometry. Determination of the transglycosylation activity of β-glucosidase in the presence of alcohols and with PNPG as a donor provided some interesting results. It is common for β-glucosidases to be activated by alcohols (Derek *et al.*, 1998), and this is largely attributed to the occurrence of transglycosylation, although in some cases it has been attributed to allosteric interaction (Gopalan *et al.*, 1989). The results in this preliminary study indicate that *D. eschscholzii* β-glucosidase shows efficiency in transferring glucose from activated donors to glucosyl acceptors. Moreover, most work on the synthesis of alkyl glucosides and related compounds has been performed using a limited range of enzymes, in particular almond (Chahid *et al.*, 1992; Ljunger *et al.*, 1994; Vic *et al.*, 1995; Panintrarux *et al.*, 1995) and *Fusarium oxysporum* (Tsimpikou *et al.*, 1996; and Makropoulou *et al.*, 1998), as well as β-glucosidases from *Aspergillus niger*, *Trichoderma reesei*, and *Candida molischiana* (Gunata *et al.*, 1994).

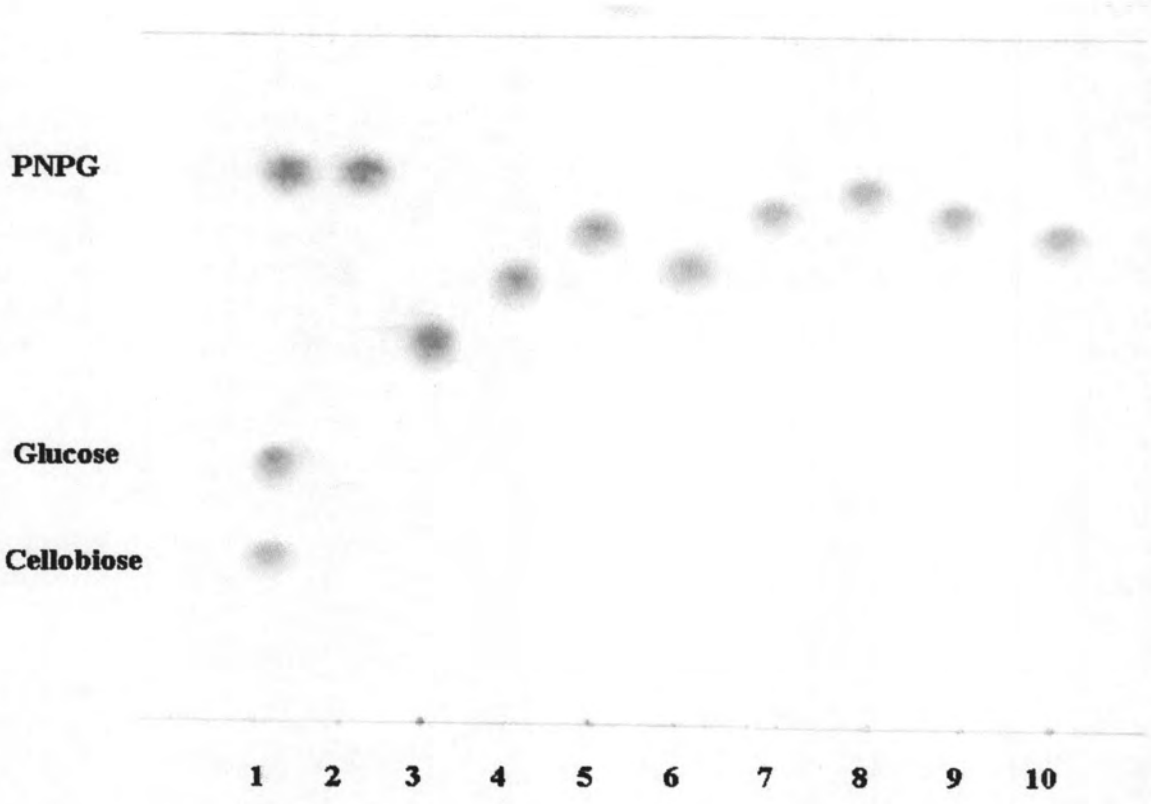

Figure 4.29 Transglucosylation of various alcohol using *D. eschscholzii* β-glucosidase by reaction with 20 mM PNPG in 0.1 M sodium acetate buffer pH 5.0 at 30 °C for 24 h. Reactions were analyzed by thin-layer chromatography on siliga gel 60 F_{254}; lane 1, standard marker containing 20 mM of PNPG, glucose, and cellobiose; lane 2, standard marker of 20 mM PNPG; lane 3-10, products from enzyme reaction between 20 mM PNPG, and 50 % (v/v) of 3: methanol; 4: ethanol; 5: *n*-propanol; 6: 2-propanol; 7: *n*-butanol; 8: 2-methyl-1-propanol; 9: 2-butanol; and 10: 2-methyl-2-propanol

4.9.2 ^{1}H NMR data

^{1}H NMR spectral data in D_2O are as follows:

Methyl-β-D-glucoside δ: 4.20 (d, 1H, H, 7.8), 3.75 (dd, 1H, 12.5, 1.6), 3.55 (dd, 2H, 12.5, 5.5), 3.40 (s, 3H), 3.29 (m, 1H), 3.20 (t, 1H, 9.36), 3.09 (t, 1H, 7.8)

Ethyl-β-D-glucoside δ: 4.29 (d, 1H, 7.8), 3.78 (m, 1H), 3.56 (m, 2H), 3.30 (m, 1H), 3.20 (t, 1H, 8.6), 3.08 (t, 3H, 8.56)

***n*-Propyl-*β*-glucoside** δ: 4.29 (d, 1H, 7.8), 3.73 (m, 1H), 3.51 (m, 2H), 3.29 (m, 1H), 3.20 (t, 1H, 9.4), 3.09 (t, 1H, 8.6), 1.46 (m, 2H), 0.75 (t, 3H, 7.02)

***n*-Butyl-β-D-glucoside** δ: 4.28 (d, 1H, 7.8), 3.76 (m, 1H), 3.53 (m, 2H), 3.26 (m, 1H), 3.08 (t, 1H, 7.8), 1.44 (m, 2H), 1.19 (m, 2H), 0.74 (t, 3H, 7.8)

2-Propyl-β-D-glucoside δ: 4.37 (d, 1H, 8.6), 3.94 (m, 1H), 3.34 (dd, 1H, 12.5, 2.3), 3.53 (m, 2H), 3.29 (m, 1H), 3.19 (dd, 1H, 9.4 3.9), 3.05 (t, 1H, 7.8), 1.07 (d, 3H, 6.2), 1.03 (d, 3H, 6.2)

2-Methyl-1-propyl-β-D-glucoside δ: 4.27 (d, 1H, 7.8), 3.74 (dd, 1H, 12.5, 1.6), 3.54 (m, 2H), 3.29 (m, 1H), 3.27 (m, 2H), 3.21 (t, 1H, 8.6), 3.10 (t, 1H, 7.8), 1.71 (m, 1H), 0.74 (t, 6H, 3.1)

2-Butyl-β-D-glucoside δ: 4.33 (d, 1H, 8.6), 3.73 (dd, 1H, 12.5, 2.3), 3.54 (m, 2H), 3.29 (m, 1H), 3.20 (t, 1H, 9.4), 3.05 (t, 1H, 9.4), 1.39 (m, 3H), 1.05 (m, 2H), 0.73 (t, 3H, 7.0)

2-Methyl-2-propyl-β-D-glucoside δ: 5.02 (d, 1H, 7.0), 3.76 (m, 1H), 3.73 (m, 1H), 3.36 (m, 2H), 3.49 (m, 1H), 3.40 (m, 1H), 1.12 (s, 6H)